

# Efficient AutoML Pipeline Search with Matrix and Tensor Factorization

Chengrun Yang, Jicong Fan, Ziyang Wu, and Madeleine Udell

This is an extended version of *AutoML Pipeline Selection: Efficiently Navigating the Combinatorial Space* (DOI: 10.1145/3394486.3403197) at the 26th ACM SIGKDD International Conference on Knowledge Discovery and Data Mining, 2020.

**Abstract**—Data scientists seeking a good supervised learning model on a new dataset have many choices to make: they must preprocess the data, select features, possibly reduce the dimension, select an estimation algorithm, and choose hyperparameters for each of these pipeline components. With new pipeline components comes a combinatorial explosion in the number of choices! In this work, we design a new AutoML system to address this challenge: an automated system to design a supervised learning pipeline. Our system uses matrix and tensor factorization as surrogate models to model the combinatorial pipeline search space. Under these models, we develop greedy experiment design protocols to efficiently gather information about a new dataset. Experiments on large corpora of real-world classification problems demonstrate the effectiveness of our approach.

**Index Terms**—AutoML, meta-learning, pipeline search, tensor factorization, matrix completion, submodular optimization, experiment design, greedy algorithms.



## 1 INTRODUCTION

A MACHINE learning pipeline is a directed graph of learning components including imputation, encoding, standardization, dimensionality reduction, and estimation, that together define a function mapping input data to output predictions. Each component may also include hyperparameters, such as the output dimension of PCA, or the number of trees in a random forest. Simple pipelines may consist of sequences of these components; more complex pipelines may combine inputs to form pipelines with more complex topologies. An example pipeline is shown as Figure 1.

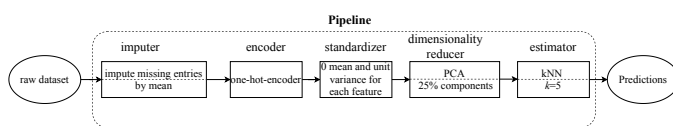


Figure 1: An example pipeline.

The job of a data scientist facing a new supervised learning problem is to choose the pipeline that yields a low out of sample error from among all possible pipelines. This task is challenging. First, no component dominates all others: there is “no free lunch” [1]. Rather, each performs well on certain data distributions. For example, the PCA dimensionality reducer works well on data points in  $\mathbb{R}^d$  that roughly lie in a low rank subspace  $\mathbb{R}^k$  with  $k < d$ ; the feature selector that keeps features with large variances works well on datasets if such features are more informative; the Gaussian naive Bayes classifier works well on features with normally

distributed values in each class. However, it is difficult to check these distributional assumptions without running the component on the data: an expensive proposition! The second is the dependence of these choices: for example, standardizing the data may help some estimators, and harm others. Moreover, as the number of possible machine learning components grows, the number of possibilities grows exponentially, defying enumeration. Automating the selection of a pipeline is thus an important problem, which has received attention both from academia and industry [2], [3], [4], [5].

Human experts tackle this difficulty by choosing the right combination according to their domain knowledge. However, finding the right combination takes substantial expertise, and still requires several model fits to find the right combination of components and hyperparameters. An automated pipeline construction system, like a human expert, first forms a *surrogate model* to predict which pipelines are likely to work well. Surrogate models are meta-models that map dataset and machine learning model properties to quantities that characterize performance or informativeness.

A good surrogate model enables efficient search through the space of pipelines. “All models are wrong, but some are useful [6]”: a good surrogate model makes predictions that guide the search for pipelines without the need for many model fits, since it is expensive to evaluate the performance of a pipeline on a large dataset. Auto-sklearn [3] uses meta-learning [7], [8], [9], [10] to choose promising pipelines from those that performed best on neighboring datasets, and uses Bayesian optimization to fine-tune hyperparameters. TPOT [2] uses genetic programming to search over pipeline topologies. Alpine Meadow [11] casts pipeline structure search as a multi-armed bandit problem and tunes model

- C. Yang, J. Fan, Z. Wu and M. Udell are with Cornell University, Ithaca, NY, 14850.  
E-mail: {cy438, jf577, zw287, udell}@cornell.edu

hyperparameters by Bayesian optimization. Our surrogate models in this paper are low rank matrices, tensors and kernelized matrices. This model makes explicit use of the combinatorial structure of the problem: as a result, the number of pipeline evaluations required to fit the surrogate model on a new dataset is modest, and independent of the number of pipeline components.

Our system learns a model for a new dataset by fitting a few pipelines on the dataset. The problem of which pipelines to evaluate first, in order to predict the effectiveness of others, is called the *cold-start problem* in the literature on recommender systems. This problem is also of great interest to the AutoML community. Proximity in meta-features, “simple, statistical or landmarking metrics to characterize datasets [12]”, are used by many AutoML systems [3], [13], [14], [15] to select models that work well on neighboring datasets, with the belief that models perform similarly on datasets with similar characteristics. Probabilistic matrix factorization has been used to extract dataset latent representations from pipeline performance [15]. Other dataset and pipeline embeddings have also been proposed: use pipeline performance or even textual dataset or algorithm descriptions to build surrogate models [12], [16], [17].

The active learning subproblem is to gain the most information to guide further model selection. Some approaches choose a function class to capture the dependence of model performance on hyperparameters; examples are Gaussian processes [15], [18], [19], [20], [21], [22], [23], [24], sparse Boolean functions [25] and decision trees [26], [27]. In this paper, our OBOE<sup>1</sup> and its extensions choose the set of multilinear models as its function class: predicted performance is linear in each of the model and dataset embeddings.

In this work, we build pipeline embeddings by fitting factorization models to the (sometimes incompletely observed) matrix or tensor of pipeline performance on a set of training datasets. These models are easy to extend to a single new dataset by fitting a constant number of pipelines on the new dataset. We describe a simple rule to select which pipelines to observe by solving a constrained version of the classical experiment design [28], [29], [30], [31] problem, using a greedy heuristic [32].

We consider the following concrete challenge: select several pipelines that perform the best within a given time limit for a new dataset, in the case that we already know or have time to collect pipeline performance on some existing datasets. What we contribute as new ideas include greedy experiment design for OBOE, a sampling model for preprocessing that takes less time for meta-training, a tensor approach as a new pipeline search mechanism, and a kernelized method that further increases accuracy. We name the system we use to search across pipelines with the same preprocessors OBOE, the system that builds on the tensor surrogate model to search across different pipeline components TENSOROBOE, and the kernelized version we have to speed up meta-training KERNELOBOE. Together, these ideas yield a state-of-the-art system for AutoML pipeline selection.

1. The eponymous musical instrument plays the initial note to tune an orchestra, which echoes our method that learn the entire space by using the knowledge from some initial evaluations.

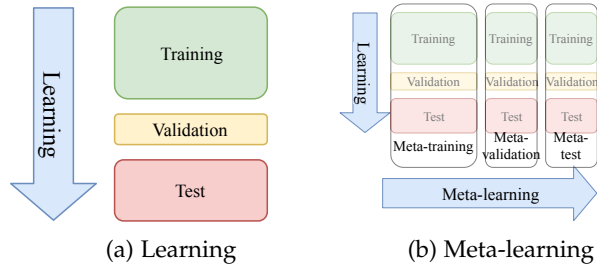


Figure 2: Standard learning vs meta-learning.

This paper is organized as follows. Section 1.1 introduces notation and terminology. Section 2 describes the main ideas we use in OBOE. Section 3 describes TENSOROBOE. Section 4 describes KERNELOBOE. Section 5 shows experimental results.

## 1.1 Notation and Terminology

**Meta-learning.** Meta-learning, also called “learning to learn”, uses results from past tasks to make predictions or decisions on a new task. In our setting, we learn from a corpus of datasets called *meta-training* datasets by fitting pipelines to these datasets in an offline stage; the new dataset, which requires a fast recommendation for a pipeline, is called the *meta-test* dataset. There can also exist *meta-validation* datasets, which are the ones we use to evaluate our pipeline recommendation method. Each of the three phases in meta-learning — meta-training, meta-validation and meta-test — is a standard learning process that includes training, validation and test, as shown in Figure 2.

**Model.** A *model*  $\mathcal{A}$  is a specific combination of algorithm and hyperparameter settings, e.g.  $k$ -nearest neighbors with  $k = 3$ .

**Pipeline component.** A pipeline component is a model or model type. Examples include missing entry imputers, dimensionality reducers, supervised learners, and data visualizers. We consider the following components in this paper:

- *Data imputer:* A preprocessor that fills in missing entries.
- *Encoder:* A transformer that converts categorical features to numerical codes. Here, we consider encoding categoricals as integers or with a one-hot encoder.
- *Standardizer:* A standardizer centers and rescales data.
- *Dimensionality reducer:* A transformer that reduces the dimensionality of the dataset by either creating new features (like PCA) or subsampling features.
- *Estimator:* The supervised learner. For the classification tasks in this paper, estimators are classifiers.

**Linear algebra.** Our paper follows the notation of [12] and [33]. We denote *vector*, *matrix*, and *tensor* variables respectively by lowercase letters ( $x$ ), capital letters ( $X$ ) and Euler script letters ( $\mathcal{X}$ ). The order of a tensor is the number of dimensions; matrices are order-two tensors. Each dimension is called a mode. Throughout this paper, all vectors are column vectors. To denote a part of matrix or tensor, we use a colon to denote the dimension that is not fixed: given a matrix  $A \in \mathbb{R}^{m \times n}$ ,  $A_{i,:}$  and  $A_{:,j}$  denote the  $i$ th row and  $j$ th column of  $A$ , respectively. A fiber is a one-dimensional section of a tensor  $\mathcal{X}$ , defined by fixing every index but one; for example, one fiber of the order-3

tensor  $\mathcal{X}$  is  $\mathcal{X}_{:jk}$ . Fibers of a tensor are analogous to rows and columns of a matrix. A slice is an  $(N - 1)$ -dimensional section of an order- $N$  tensor  $\mathcal{X}$ . The mode- $n$  matricization of  $\mathcal{X}$ , denoted as  $\mathcal{X}^{(n)}$ , is a matrix whose columns are the mode- $n$  fibers of  $\mathcal{X}$ . For example, given an order-3 tensor  $\mathcal{X} \in \mathbb{R}^{I \times J \times K}$ ,  $\mathcal{X}^{(1)} \in \mathbb{R}^{I \times (J \times K)}$ . We denote the  $n$ -mode product of a tensor  $\mathcal{X} \in \mathbb{R}^{I_1 \times I_2 \times \dots \times I_N}$  with a matrix  $U \in \mathbb{R}^{J \times I_n}$  by  $\mathcal{X} \times_n U \in \mathbb{R}^{I_1 \times \dots \times I_{n-1} \times J \times I_{n+1} \times \dots \times I_N}$ ; the  $(i_1, i_2, \dots, i_{n-1}, j, i_{n+1}, \dots, i_N)$ -th entry is  $\sum_{i_n=1}^{I_n} x_{i_1 i_2 \dots i_{n-1} i_n i_{n+1} \dots i_N} u_{j i_n}$ . Given two tensors with the same shape, we use  $\odot$  to denote their entrywise product. We define  $[n] = \{1, \dots, n\}$  for  $n \in \mathbb{Z}$ . Given an ordered set  $\mathcal{S} = \{s_1, \dots, s_k\}$  where  $s_1 < \dots < s_k \in [n]$ , we write  $A_{:\mathcal{S}} = [A_{:,s_1}, A_{:,s_2}, \dots, A_{:,s_k}]$ ; given an ordinary set  $S$ , we use  $A_{:S}$  to denote  $A_{:\mathcal{S}'}$ , in which  $\mathcal{S}'$  is the ordered version of set  $S$ . The Frobenius norm of a tensor  $\mathcal{X} \in \mathbb{R}^{I_1 \times I_2 \times \dots \times I_N}$  is  $\|\mathcal{X}\|_F = \sqrt{\sum_{i_1 \in [I_1], i_2 \in [I_2], \dots, i_N \in [I_N]} x_{i_1 i_2 \dots i_N}^2}$ .

**Pipeline performance.** The performance of a machine learning pipeline is usually characterized by cross-validation error. Given a dataset  $\mathcal{D}$  and a pipeline  $\mathcal{P}$ , we denote the error of  $\mathcal{P}$  on  $\mathcal{D}$  as  $\mathcal{P}(\mathcal{D})$ . It is common practice to evaluate this error by cross-validating  $\mathcal{P}$  on  $\mathcal{D}$  with a certain number of folds (often 3, 5 or 10) and a fixed dataset partition. We use  $\mathcal{P}(\mathcal{D})$  to denote the cross-validation error we observe with a certain number of folds and a certain partition.

**Error tensor and error matrix.** Pipeline errors on training datasets form an *error tensor*, which we denote as  $\mathcal{E}$ . In our experiments,  $\mathcal{E}$  is an order-6 tensor, with 6 modes corresponding to datasets, imputers, encoders, standardizers, dimensionality reducers and estimators, respectively. The  $(i_1, i_2, \dots, i_6)$ -th entry of  $\mathcal{E}$  is the error of the pipeline formed by composing the  $i_2$ -th imputer,  $i_3$ -th encoder,  $i_4$ -th standardizer,  $i_5$ -th dimensionality reducer, and  $i_6$ -th estimator and evaluating this pipeline on the  $i_1$ -th dataset. If a pipeline-dataset combination has been evaluated, we say the corresponding entry in the error tensor  $\mathcal{E}$  is observed. The first unfolding of the error tensor,  $\mathcal{E}^{(1)}$ , is called the *error matrix*  $E$ , whose  $ij$ th entry  $E_{ij} = \mathcal{P}_j(\mathcal{D}_i)$  is the error of pipeline  $j$  on dataset  $i$ .

**Time target and time budget.** The time target refers to the anticipated time spent running models to infer latent features of each fixed dimension and can be exceeded. However, the runtime does not usually deviate much from the target since our model runtime prediction works well. The time budget refers to the total time limit for OBOE and is never exceeded.

**Ensemble.** An ensemble [34], [35], [36], [37] combines a finite set of individual machine learning models into a single prediction model. For simplicity, the combination method we use is majority voting for classification. We define the *candidate learner* to be individual machine learning pipelines that we select from to create the ensemble, and *base learner* to be pipelines that are included in the ensemble. An ensemble of pipelines is itself a pipeline, but not a simple linear pipeline. By creating ensembles of linear pipelines, our system can perform better than any linear pipeline.

## 2 OBOE

OBOE selects among a set of machine learning estimators, and build pipelines with the same set of preprocessors. This is because the estimator is usually the most crucial part of a pipeline and is what practitioners usually spend a large amount of resources to choose. However, the method described here is not limited to choosing among estimators; it is able to choose among machine learning models in general.

### 2.1 Overview

Shown in Figure 3, the meta-learning system for estimator selection, OBOE, has two phases. In the *offline* phase, we compute the performance of estimators on meta-training datasets and compute a surrogate model. In the *online* phase, we run a small number of estimators on the new meta-test dataset to help infer the performance of the rest. The offline phase is executed only once and explores the space of estimator performance on meta-training datasets. Time taken in this phase does not affect the runtime of OBOE on a new dataset; the runtime experienced by user is that of the online phase.

One advantage of OBOE is that the vast majority of the time in the online phase is spent training standard machine learning models, while very little time is required to decide which models to sample. Training these standard machine learning models requires running algorithms on datasets with thousands of data points and features, while the meta-learning task — deciding which models to sample — requires only solving a small least-squares problem.

#### 2.1.1 Offline Stage

The  $(i, j)$ th entry of error matrix  $E \in \mathbb{R}^{m \times n}$  in OBOE, denoted as  $E_{ij}$ , records the performance of the  $j$ th estimator on the  $i$ th meta-training dataset. We collect the error matrix using the *balanced error rate* metric, the average of false positive and false negative rates across different classes. At the same time we record runtime of estimators on datasets. This is used to fit runtime predictors that will be addressed in Section 2.3. Pseudocode for the offline phase is shown as Algorithm 1.

---

#### Algorithm 1 Offline Stage

---

**Input:** meta-training datasets  $\{\mathcal{D}_i\}_{i=1}^m$ , estimators  $\{\mathcal{A}_j\}_{j=1}^n$ , algorithm performance metric  $\mathcal{M}$

**Output:** error matrix  $E$ , runtime matrix  $T$ , fitted runtime predictors  $\{f_j\}_{j=1}^n$

```

1 for  $i = 1, 2, \dots, m$  do
2    $n^{\mathcal{D}_i}, p^{\mathcal{D}_i} \leftarrow$  number of data points and features in  $\mathcal{D}_i$ 
3   for  $j = 1, 2, \dots, n$  do
4      $E_{ij} \leftarrow$  error of model  $\mathcal{A}_j$  on dataset  $\mathcal{D}_i$  according
      to metric  $\mathcal{M}$ 
5      $T_{ij} \leftarrow$  observed runtime for model  $\mathcal{A}_j$  on dataset
       $\mathcal{D}_i$ 
6 for  $j = 1, 2, \dots, n$  do
7   fit  $f_j = \text{fit\_runtime}(n, p, T_j)$  (Section 2.3)

```

---

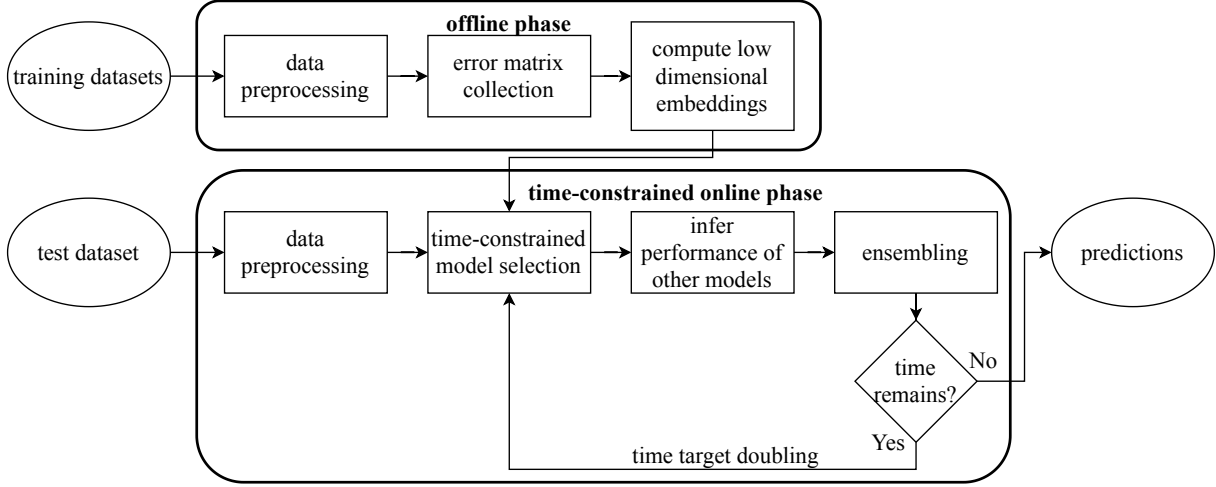


Figure 3: Diagram of data processing flow in the OBOE system.

### 2.1.2 Online Stage

We repeatedly double the time target of each round until we use up the total time budget. Each round is a subroutine of the entire online stage and is shown as Algorithm 2.

- Time-constrained model selection** Our active learning procedure selects a fast and informative collection of estimators to run on the meta-test dataset. OBOE uses the results of these fits to estimate the performance of all other models as accurately as possible. The procedure is as follows. First predict estimator runtime on the meta-test dataset using fitted runtime predictors. Then use experiment design to select a subset  $\mathcal{S}$  of entries of  $e$ , the performance vector of the test dataset, to observe. The observed entries are used to compute  $\hat{x}$ , an estimate of the latent meta-features of the test dataset, which in turn is used to predict every entry of  $e$ . We build an ensemble out of pipelines predicted to perform well within the time target  $\tilde{\tau}$ . This subroutine  $\tilde{A} = \text{ensemble\_selection}(\mathcal{S}, e_{\mathcal{S}}, z_{\mathcal{S}})$  takes as input the set of base learners  $\mathcal{S}$  with their cross-validation errors  $e_{\mathcal{S}}$  and predicted labels  $z_{\mathcal{S}} = \{z_s | s \in \mathcal{S}\}$ , and outputs ensemble learner  $\tilde{A}$ . The hyperparameters used by models in the ensemble can be tuned further, but in our experiments we did not observe substantial improvements from further hyperparameter tuning.
- Time target doubling** To select rank  $k$ , OBOE starts with a small initial rank along with a small time target, and then doubles the time target for `fit_one_round` until the elapsed time reaches half of the total budget. The rank  $k$  increments by 1 if the validation error of the ensemble learner decreases after doubling the time target, and otherwise does not change. Since the matrices returned by PCA with rank  $k$  are submatrices of those returned by PCA with rank  $l$  for  $l > k$ , we can compute the factors as submatrices of the  $m$ -by- $n$  matrices returned by PCA with full rank  $\min(m, n)$  [38]. The pseudocode is shown as Algorithm 3.

## 2.2 Pipeline Performance Prediction

It can be difficult to determine *a priori* which meta-features to use so that algorithms perform similarly well on datasets

### Algorithm 2 Online phase, single round

**Input:** model latent meta-features  $\{y_j\}_{j=1}^n$ , fitted runtime predictors  $\{f_j\}_{j=1}^n$ , training fold of the meta-test dataset  $\mathcal{D}_{\text{tr}}$ , number of best models  $N$  to select from the estimated performance vector, time target for this round  $\tilde{\tau}$

**Output:** ensemble learner  $\tilde{A}$

```

1 function FIT_ONE_ROUND
2   for  $j = 1, 2, \dots, n$  do
3      $\hat{t}_j \leftarrow f_j(n^{\mathcal{D}_{\text{tr}}}, p^{\mathcal{D}_{\text{tr}}})$ 
4    $\mathcal{S} = \text{min\_variance\_ED}(\hat{t}, \{y_j\}_{j=1}^n, \tilde{\tau})$ 
5   for  $k = 1, 2, \dots, |\mathcal{S}|$  do
6      $e_{\mathcal{S}_k} \leftarrow$  cross-validation error of model  $\mathcal{A}_{\mathcal{S}_k}$  on  $\mathcal{D}_{\text{tr}}$ 
7      $\hat{x} \leftarrow ([y_{\mathcal{S}_1} \ y_{\mathcal{S}_2} \ \dots \ y_{\mathcal{S}_{|\mathcal{S}|}}]^\top)^\dagger e_{\mathcal{S}}$ 
8      $\hat{e} \leftarrow [y_1 \ y_2 \ \dots \ y_n]^\top \hat{x}$ 
9      $\mathcal{T} \leftarrow$  the  $N$  models with lowest predicted errors in  $\hat{e}$ 
10    for  $k = 1, 2, \dots, |\mathcal{T}|$  do
11       $e_{\mathcal{T}_k}, z_{\mathcal{T}_k} \leftarrow$  cross-validation error of model  $\mathcal{A}_{\mathcal{T}_k}$ 
12    on  $\mathcal{D}_{\text{tr}}$ 
13     $\tilde{A} \leftarrow \text{ensemble\_selection}(\mathcal{T}, e_{\mathcal{T}}, z_{\mathcal{T}})$ 
  
```

with similar meta-features. Also, the computation of some landmarking meta-features can be expensive. To infer model performance on a dataset without any expensive meta-feature calculations, we use collaborative filtering to infer latent meta-features for datasets.

As shown in Figure 4, we construct an empirical error matrix  $E \in \mathbb{R}^{m \times n}$ , where every entry  $E_{ij}$  records the cross-validated error of model  $j$  on dataset  $i$ . Empirically,  $E$  has approximately low rank: Figure 5 shows the singular values  $\sigma_i(E)$  decay rapidly as a function of the index  $i$ . This observation serves as foundation of our algorithm. The value  $E_{ij}$  provides a noisy but unbiased estimate of the true performance of a model on the dataset:  $\mathbb{E}E_{ij} = \mathcal{A}_j(\mathcal{D}_i)$ .

To denoise this estimate, we approximate  $E_{ij} \approx x_i^\top y_j$  where  $x_i$  and  $y_j$  minimize  $\sum_{i=1}^m \sum_{j=1}^n (E_{ij} - x_i^\top y_j)^2$  with  $x_i, y_j \in \mathbb{R}^k$  for  $i \in [M]$  and  $j \in [N]$ ; the solution is given by PCA. Thus  $x_i$  and  $y_j$  are the latent meta-features of dataset  $i$  and model  $j$ , respectively. The rank  $k$  controls model fidelity: small  $k$ s give coarse approximations, while

---

**Algorithm 3** Online Stage
 

---

**Input:** error matrix  $E$ , runtime matrix  $T$ , meta-test dataset  $\mathcal{D}$ , total time budget  $\tau$ , fitted runtime predictors  $\{f_j\}_{j=1}^n$ , initial time target  $\tilde{\tau}_0$ , initial approximate rank  $k_0$

**Output:** ensemble learner  $\tilde{A}$

```

1 function ENSEMBLE_SELECTION
2    $x_i, y_j \leftarrow \arg \min \sum_{i=1}^m \sum_{j=1}^n (E_{ij} - x_i^\top y_j)^2$ ,  $x_i \in \mathbb{R}^{\min(m,n)}$  for  $i \in [M]$ ,  $y_j \in \mathbb{R}^{\min(m,n)}$  for  $j \in [N]$ 
3    $\mathcal{D}_{\text{tr}}, \mathcal{D}_{\text{val}}, \mathcal{D}_{\text{te}} \leftarrow$  training, validation and test folds of  $\mathcal{D}$ 
4    $\tilde{\tau} \leftarrow \tilde{\tau}_0$ 
5    $k \leftarrow k_0$ 
6   while  $\tilde{\tau} \leq \tau/2$  do
7      $\{\tilde{y}_j\}_{j=1}^n \leftarrow k$ -dimensional subvectors of  $\{y_j\}_{j=1}^n$ 
8      $\tilde{A} \leftarrow \text{fit\_one\_round}(\{\tilde{y}_j\}_{j=1}^n, \{f_j\}_{j=1}^n, \mathcal{D}_{\text{tr}}, \tilde{\tau})$ 
9      $e'_{\tilde{A}} \leftarrow \tilde{A}(\mathcal{D}_{\text{val}})$ 
10    if  $e'_{\tilde{A}} < e_{\tilde{A}}$  then
11       $k \leftarrow k + 1$ 
12     $\tilde{\tau} \leftarrow 2\tilde{\tau}$ 
13     $e_{\tilde{A}} \leftarrow e'_{\tilde{A}}$ 
14  return  $\tilde{A}$ 

```

---

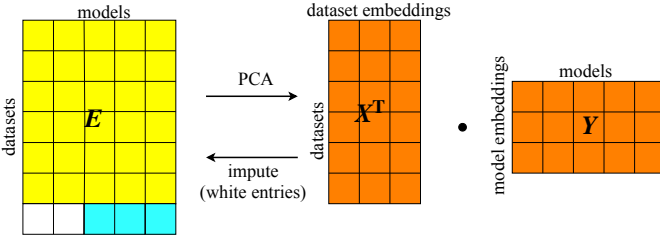


Figure 4: Model performance prediction by the error matrix  $E$  (yellow blocks only). Perform PCA on the error matrix (offline) to compute dataset ( $X$ ) and model ( $Y$ ) embeddings (orange blocks). Given a new dataset (row with white and blue blocks), pick a subset of models to observe (blue blocks). Use  $Y$  together with the observed models to impute the performance of the unobserved models on the new dataset (white blocks).

large  $k$ s may overfit. We use a doubling scheme to choose  $k$  within time budget; see Section 2.1.2 for details.

Given a new meta-test dataset, we choose a subset  $S \subseteq [N]$  of models and observe performance  $e_j$  of model  $j$  for each  $j \in S$ . A good choice of  $S$  balances information gain against time needed to run the models; we discuss how to choose  $S$  in Section 2.4. We then infer latent meta-features for the new dataset by solving the least squares problem: minimize  $\sum_{j \in S} (e_j - \hat{x}^\top y_j)^2$  with  $\hat{x} \in \mathbb{R}^k$ . For all unobserved models, we predict their performance as  $\hat{e}_j = \hat{x}^\top y_j$  for  $j \notin S$ .

### 2.3 Runtime Prediction

Estimating model runtime allows us to trade off between running slow, informative models and fast, less informative models. We use a simple method to estimate runtimes, using polynomial regression on  $n^{\mathcal{D}}$  and  $p^{\mathcal{D}}$ , the numbers of data points and features in  $\mathcal{D}$ , and their logarithms, since

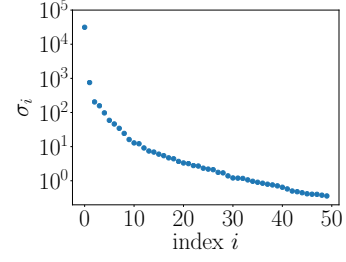


Figure 5: Singular value decay of an error matrix. The entries are calculated by 5-fold cross validation of machine pipelines (listed in Appendix A, Table 2) with fixed components except estimators, on meta-training OpenML datasets (list in Appendix A.1).

the theoretical complexities of machine learning algorithms we use are  $O((n^{\mathcal{D}})^3, (p^{\mathcal{D}})^3, (\log(n^{\mathcal{D}}))^3)$ . Hence we fit an independent polynomial regression model for each model:

$$f_j = \operatorname{argmin}_{f_j \in \mathcal{F}} \sum_{i=1}^M \left( f_j(n^{\mathcal{D}_i}, p^{\mathcal{D}_i}, \log(n^{\mathcal{D}_i})) - t_j^{\mathcal{D}_i} \right)^2, j \in [n]$$

where  $t_j^{\mathcal{D}}$  is the runtime of machine learning model  $j$  on dataset  $\mathcal{D}$ , and  $\mathcal{F}$  is the set of all polynomials of order no more than 3. We denote this procedure by  $f_j = \text{fit\_runtime}(n, p, t)$ .

We observe that this model predicts runtime within a factor of two for half of the machine learning models on more than 75% meta-training OpenML datasets, and within a factor of four for nearly all models, as shown in Section 5.4.

### 2.4 Fast and Accurate Resource-Constrained Active Learning

The methodology we describe here applies to not only machine learning estimators but also other models and pipelines in general.

Given a new dataset, our first problem is to select a subset of pipelines to fit, so that we may estimate the performance of other pipelines. We use ideas from linear experiment design, which picks a subset of low-cost statistical trials to minimize the variance of the resulting estimator, to make this selection.

Concretely, we estimate the embedding  $x$  of the new dataset by linear regression. Given the linear model as Equation 8, given known performance  $e_S$  of a subset  $S \subseteq [n]$  of pipelines on the new dataset, we have

$$e_S = (Y_{:S})^\top x + \epsilon \quad (1)$$

in which  $Y$  collects the latent embeddings of pipeline performance, and  $\epsilon$  is the error in this linear model. For example, the error may be due to misspecification of the low Tucker factorization model for the error tensor. We estimate  $x$  by linear regression and denote the result as  $\hat{x}$ . Then we estimate the performance of pipelines in  $[n] \setminus S$  by the corresponding entries in  $\hat{e} = Y^\top \hat{x}$ .

Now we consider which  $S$  to choose to accurately estimate  $x$ . Suppose the error  $\epsilon \sim \mathcal{N}(0, \sigma^2 I)$ . Using the linear regression model, Equation 1, we want to minimize the expected  $\ell_2$  error  $E_\epsilon \|\hat{x} - x\|^2 = E_\epsilon \|\hat{x} - E_\epsilon \hat{x}\|^2 + \|E_\epsilon \hat{x} - x\|^2$ .

Here, the second term is 0 since linear regression is unbiased, and the first term is the covariance  $\sigma^2(Y Y^\top)^{-1}$  of the estimated embedding  $\hat{x}$ , which is straightforward to compute.

We will first show how to constrain the *number* of sampled pipelines. Imagine we have enough time to run at most  $m$  pipelines (and all pipelines run equally slowly). Given pipeline embeddings  $\{y_j\}_{j=1}^n$  (which we call *design vectors* or *designs*), in which each  $y_j \in \mathbb{R}^k$ , we minimize a scalarization of the covariance to obtain the (number-constrained)  $D$ -optimal experiment design problem

$$\begin{aligned} & \text{maximize} && \log \det \left( \sum_{j \in S} y_j y_j^\top \right) \\ & \text{subject to} && |S| \leq m \\ & && S \subseteq [n]. \end{aligned} \quad (2)$$

Here,  $\sum_{j \in S} y_j y_j^\top$ , the inverse of (scaled) covariance matrix, is called the Fisher information matrix.

Obtaining an exact solution for a mixed-integer nonlinear optimization problem like Problem 2 is prohibitively expensive. People have thus developed a variety of approaches to solve Problem 2 to certain accuracy, including convexification, greedy, local search, etc. We will show the convexification approach in Section 2.4.1, the greedy approach in Section 2.4.2, and then develop a *time*-constrained version that we use in practice in Section 2.4.3.

#### 2.4.1 Convexification method for size-constrained experiment design

Convexification is commonly used to solve a mixed-integer problem that can be easily transformed to a convex optimization by relaxation [12], [30], [31].

Define an indicator vector  $v \in \{0, 1\}^n$ , where entry  $v_j$  indicates whether to fit model  $j$ . Problem 2 is thus equivalent to the following formulation with variable  $v \in \mathbb{R}^n$ :

$$\begin{aligned} & \text{minimize} && \log \det \left( \sum_{j=1}^n v_j y_j y_j^\top \right)^{-1} \\ & \text{subject to} && \sum_{j=1}^n v_j \leq m \\ & && v_j \in \{0, 1\}, \forall j \in [n] \end{aligned} \quad (3)$$

Now relax to allow  $v \in [0, 1]^n$  to allow for non-Boolean values and get the convex version for Problem 3, and solve by a convex solver. To binarize the solution, we may either choose the set of  $m$  entries with largest values as  $S$ , or truncate at a certain threshold.

#### 2.4.2 Greedy method for size-constrained experiment design

In practice, there may be a large number of models in our model selection problem, commonly at least tens of thousands. The convexification method is too slow in that case. Also, the convexification method does not have suboptimality guarantee. Moreover, we can find better solutions with the greedy heuristic we present next.

Greedy methods form another popular approach to combinatorial optimization problems like Problem 2. Importantly, the objective function of Problem 2,  $f(S) = \log \det \left( \sum_{j \in S} y_j y_j^\top \right)$ , is submodular. (Recall a set function  $g : 2^V \rightarrow \mathbb{R}$  defined on a subset of  $V$  is submodular if for every  $A \subseteq B \subseteq V$  and every element  $s \in V \setminus B$ , we have

$g(A \cup \{s\}) - g(A) \geq g(B \cup \{s\}) - g(B)$ . This characterizes a ‘‘diminishing return’’ property.) Given a size constraint, the submodular function maximization problem

$$\begin{aligned} & \text{maximize} && g(S) \\ & \text{subject to} && S \subseteq V \\ & && |S| \leq m \end{aligned} \quad (4)$$

can be solved with a  $1 - \frac{1}{e}$  approximation ratio [39] by the greedy approach: in every step, add the single element that maximizes the increase in function value [40], [41], [42]. In  $D$ -optimal experiment design, we can compute this increase efficiently using Lemma 2.1.

**Lemma 2.1 (Matrix Determinant Lemma [32], [43]).** For any invertible matrix  $A \in \mathbb{R}^{k \times k}$  and  $a, b \in \mathbb{R}^k$ ,

$$\det(A + ab^\top) = \det(A)(1 + b^\top A^{-1}a)$$

At the  $t$ -th step in our setting, with an already constructed Fisher information matrix  $X_t = \sum_{j \in S} y_j y_j^\top$ , we have

$$\arg \max_{j \in [n] \setminus S} \det(X_t + y_j y_j^\top) = \arg \max_{j \in [n] \setminus S} y_j^\top X_t^{-1} y_j. \quad (5)$$

Here,  $y_j^\top X_t^{-1} y_j$  can be seen as the payoff for adding pipeline  $j$ . From the  $t$ -th to the  $(t+1)$ -th step, with the selected design vector at the  $t$ -th step as  $y_i$ , we can update  $X_t$  to  $X_{t+1} = (X_t + y_i y_i^\top)$  by Lemma 2.2:

**Lemma 2.2 (Sherman-Morrison formula [44], [45]).** For any invertible matrix  $A \in \mathbb{R}^{k \times k}$  and  $a, b \in \mathbb{R}^k$ ,

$$(A + ab^\top)^{-1} = A^{-1} - \frac{A^{-1}ab^\top A^{-1}}{1 + b^\top A^{-1}a}$$

Pseudocode for the greedy algorithm for Problem 2 is shown as Algorithm 4, with per-iteration time complexity  $O(k^3 + nk^2)$ : it takes  $O(k^3)$  (for a naive matrix multiplication algorithm) to update  $X_t^{-1}$  and  $O(nk^2)$  to choose the best pipeline to add.

---

**Algorithm 4** Greedy algorithm for size-constrained  $D$ -design

---

**Input:** design vectors  $\{y_j\}_{j=1}^n$ , in which  $y_j \in \mathbb{R}^k$ ; maximum number of selected pipelines  $m$ ; initial set of designs  $S_0 \subseteq [n]$ , s.t.  $X_0 = \sum_{j \in S_0} y_j y_j^\top$  is non-singular

**Output:** The selected set of designs  $S \subseteq [n]$

```

1  function GREEDY_ED_NUMBER
2  do
3      S ← S0
4      i ← argmaxj ∈ [n] \ S yj⊤ Xt−1 yj
5      S ← S ∪ {i}
6      Xt+1 ← Xt + yi yi⊤
7      Xt+1−1 ← Sherman_Morrison(Xt, yi)
8  while |S| ≤ m
9  return S
```

---

There remains the problem of how to select an initial set of designs  $S$  to start from, such that  $X_0 = \sum_{j \in S} y_j y_j^\top = Y_S Y_S^\top$  is non-singular. This is equivalent to the problem of finding a subset of vectors in  $\{y_j\}_{j=1}^n$  that can span  $\mathbb{R}^k$ . We select this sized- $k$  subset  $S_0$  to be the first  $k$  pivot columns from QR factorization with column pivoting [38], [46] on  $Y$ , with time complexity  $O((n+k)k^2)$ .

### 2.4.3 Greedy method for time-constrained experiment design

We here move on to the realistic case that we face in AutoML pipeline selection: which pipelines should we select to gain an accurate estimate of the entire pipeline space? In this setting, each pipeline is associated with a different cost. We characterize the cost as running time, and form the time-constrained version of experiment design as

$$\begin{aligned} & \text{maximize} && \log \det \left( \sum_{j \in S} y_j y_j^\top \right) \\ & \text{subject to} && \sum_{j \in S} \hat{t}_j \leq \tau \\ & && S \subseteq [n], \end{aligned} \quad (6)$$

in which  $\{\hat{t}_i\}_{i=1}^n$  are the estimated pipeline running times,  $\tau$  is the runtime limit. The payoff of adding design  $j$  in the  $t$ -th step can thus be formulated as  $\frac{y_j^\top X_t^{-1} y_j}{\hat{t}_j}$ . We have as Algorithm 5 the greedy method to solve Problem 6.

---

**Algorithm 5** Greedy algorithm for time-constrained  $D$ -design

---

**Input:** design vectors  $\{y_j\}_{j=1}^n$ , in which  $y_j \in \mathbb{R}^k$ ; estimated running time of all pipelines  $\{\hat{t}_i\}_{i=1}^n$ ; maximum running time  $\tau$ ; initial set of designs  $S_0 \subseteq [n]$ , s.t.  $X_0 = \sum_{j \in S_0} y_j y_j^\top$  is non-singular

**Output:** The selected set of designs  $S \subseteq [n]$

```

1  function GREEDY_ED_TIME
2  do
3      S ← S0
4      i ← argmaxj ∈ [n] \ S  $\frac{y_j^\top X_t^{-1} y_j}{\hat{t}_j}$ 
5      S ← S ∪ {i}
6      Xt+1 ← Xt + yi yi⊤
7  while  $\sum_{i \in S} \hat{t}_i \leq \tau$ 
8  return S
```

---

The initialization problem is solved similarly by the QR method. Given runtime limit  $\tau$ , we select among columns with corresponding pipelines predicted to finish within  $\frac{\tau}{2k}$ . Pseudocode for this initialization algorithm is shown as Algorithm 6.

A corner case of Algorithm 6, shown as Case 1, is that there are not enough pipelines predicted to be able to finish within time limit. This corresponds to the case that the runtime limit is relatively small compared to the time of fitting pipelines on current dataset. In this case we greedily select the fast pipelines and do not run Algorithm 5 afterwards.

As a side note, the assumption that performance of different pipelines are predicted with equal variance is not quite realistic, especially when some components have much more pipelines than others. If the variance is known (but unequal), we obtain a weighted least squares problem. In the error matrix  $E$ , we can estimate the variance of prediction error of each pipeline  $j \in [n]$  by the sample variance of  $E_{:,j} - X^\top Y_{:,j}$  and select the promising pipelines with the goal of minimizing the rescaled covariance. Practically, however, this rescaled method does not systematically improve on the standard least squares approach in our experiments (shown in Appendix C), so we retrench to the simpler approach.

---

**Algorithm 6** Initialization of the greedy algorithm for time-constrained  $D$ -design, by QR factorization with column pivoting

---

**Input:** design vectors  $\{y_j\}_{j=1}^n$ , in which  $y_j \in \mathbb{R}^k$ ; (predicted) running time of all pipelines  $\{\hat{t}_i\}_{i=1}^n$ ; maximum running time  $\tau$

**Output:** A subset of designs  $S_0 \subseteq [n]$  for Algorithm 5 initialization

```

1  function QR_INITIALIZATION
2      Svalid ← {i ∈ [n] :  $\hat{t}_i \leq \frac{\tau}{2k}$ }
3      S0 ← ∅,  $\hat{t}_{\text{sum}} \leftarrow 0$ 
4  if |Svalid| < k then ▷ Case 1
5      do
6          i ← argminj ∈ [n] \ S  $\hat{t}_j$ 
7          S0 ← S0 ∪ {i}
8           $\hat{t}_{\text{sum}} \leftarrow \hat{t}_{\text{sum}} + \hat{t}_j$ 
9  while  $\hat{t}_{\text{sum}} \leq \tau$ 
10 else ▷ Case 2
11     S0 ← QR_with_column_pivoting(YSvalid)[ : k]
12 return S0
```

---

## 3 TENSOROBOE

OBOE focuses on the selection of machine learning estimators. In practice, preprocessors also have a large influence on model quality; the selection of which incurs high cost as well. In this section, to model and utilize the combinatorial structure among pipeline components, we move on to the AutoML system for selecting among pipelines with different imputers, dimensionality reducers, estimators, etc. The name TENSOROBOE comes from the tensor surrogate model we use. As we will demonstrate by calculation in Section 3.4 and by experiments in Section 5.2, the tensor model is better at modeling the combinatorial structure of pipeline components than matrices from tensor matricization.

### 3.1 Overview

TENSOROBOE has two phases that are similar to those of OBOE. In the offline phase, we compute the performance of pipelines on meta-training datasets and compute a surrogate model. In the online phase, we run a small number of pipelines on the new meta-test dataset to specialize the surrogate model and identify promising pipelines.

**Offline Stage.** We collect a partially observed error tensor using the approach described in Section 3.2 to limit the total runtime of the offline phase. We complete and factorize the error tensor  $\mathcal{E}$  using the EM-Tucker algorithm, shown as Algorithm 7, with dataset and estimator ranks empirically chosen to be the ones that give low reconstruction error, described in Section 5.2.

**Online Stage.** Online, given a new dataset  $\mathcal{D}$  with  $n^{\mathcal{D}}$  data points and  $p^{\mathcal{D}}$  features, we first predict the running time of each pipeline by a simple model: order-3 polynomial regression on  $n^{\mathcal{D}}$  and  $p^{\mathcal{D}}$  and their logarithms. This simple model works well because the time to fit the estimator dominates the time to fit the pipeline, and the theoretical complexities of estimators we use have no higher order terms [12], [47].

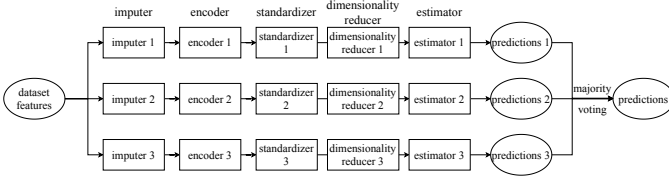


Figure 6: A pipeline ensemble with 3 base learners.

The initial dataset and estimator ranks are set to the number of principal components that capture 97% of the energy in the respective tensor matricizations. We double the runtime budget at each iteration and increment the estimator rank if the performance improves. In each iteration, we select informative pipelines by formulating the time-constrained experiment design problem as Problem 6 and solve by the greedy approach as Algorithm 5. Then we build ensembles whose base learners are the 5 pipelines with the best cross-validation error. An ensemble can improve on the performance of the best base pipeline. An example is shown as Figure 6.

### 3.2 Tensor Collection for Meta-Training

In the meta-training phase of meta-learning, meta-training data is generally assumed to be already available or cheap to collect. Given the large number of possible pipeline combinations, though, collecting meta-training data can be prohibitively expensive. As an example, even if it takes one minute on average to evaluate each pipeline on each dataset, evaluating 20,000 pipelines on 200 meta-training datasets would take more than 7 years of CPU time. This motivates us to use tensor completion to limit the time spent collecting meta-training data efficiently while preserving accuracy of our surrogate model.

We collect pipeline performance in a biased way: using 3-fold cross-validation, we only evaluate pipelines that complete within 120 seconds. This rule gives a missing ratio of 3.3%. Notice that the entries are not missing uniformly at random: for example, some datasets are large and expensive to evaluate; our training data systematically lacks data from these large datasets. Nevertheless, we will show how to infer these entries using tensor completion in Section 3.3, and demonstrate in Section 5.2 that the method performs well despite bias.

### 3.3 Tensor Factorization and Rank

The meta-training phase constructs the error tensor  $\mathcal{E}$ . In the meta-test phase, we see a new dataset, corresponding to a new slice of  $\mathcal{E}$ . To learn about the slice efficiently, use a low rank tensor factorization to predict all the entries in this slice from a subset of informative entries

Unlike matrices, there are many incompatible notions of tensor rank and low rank tensor decompositions, including CANDECOMP/PARAFAC (CP) [48], [49], Tucker [50], and tensor-train [51]. Each emphasizes a different aspect of the tensor low rank property.

In this paper, we use Tucker decomposition; an example on an order-3 tensor is shown as Figure 7. As a form of higher-order PCA, Tucker decomposes a tensor into the

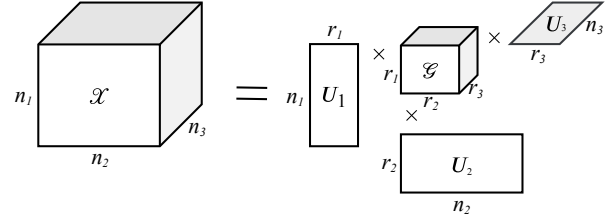


Figure 7: Tucker decomposition on an order-3 tensor.

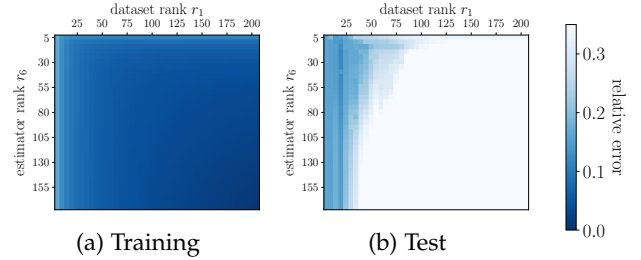


Figure 8: Relative error heatmaps when varying ranks in dataset and estimator dimensions. Here, training entries are the ones with runtime less than 90 seconds; the test entries are the ones with runtime between 90 and 120 seconds.

product of a *core tensor* and several *factor matrices*, one for each mode [33]. In our setting of order-6 tensors, Tucker decomposition of  $\mathcal{E}$  is

$$\mathcal{E} \approx \hat{\mathcal{E}} = \mathcal{G} \times_1 U_1 \times \cdots \times_6 U_6 \quad (7)$$

with core tensor  $\mathcal{G} \in \mathbb{R}^{r_1 \times r_2 \times \cdots \times r_6}$  and factor matrices  $U_i \in \mathbb{R}^{n_i \times r_i}$ ,  $i \in \{1, 2, \dots, 6\}$  with orthonormal columns. Each factor matrix corresponds to the respective pipeline component;  $\hat{\mathcal{E}}$  is linear in the factor matrices. Each factor matrix can thus be viewed as embedding the corresponding pipeline component, with pipeline embeddings as columns of  $Y = (\mathcal{G} \times_2 U_2 \times \cdots \times_6 U_6)_1 \in \mathbb{R}^{r_1 \times (\prod_{i=2}^6 n_i)}$ , the mode-1 matricization of the product. We can use this observation to approximately factor the error matrix  $E$ , using Equation 7, as

$$X^\top Y \approx E \in \mathbb{R}^{n_1 \times (\prod_{i=2}^6 n_i)} \quad (8)$$

in which  $X \in \mathbb{R}^{r_1 \times n_1}$  and  $Y \in \mathbb{R}^{r_1 \times (\prod_{i=2}^6 n_i)}$  are dataset and pipeline embeddings, respectively.

We evaluate the factorization performance by relative error, defined as  $\|\Omega \odot (X - \hat{X})\|_F^2 / \|\Omega \odot X\|_F^2$ :  $X$  is the true tensor,  $\hat{X}$  is the predicted tensor, and  $\Omega$  is a binary tensor that has the same shape as  $X$  and  $\hat{X}$ .  $\Omega_{i_1, i_2, \dots, i_6} = 1$  if the  $(i_1, i_2, \dots, i_6)$ -th entry is in the set of entries we care about, and 0 otherwise.

Figure 8 shows the low Tucker rank factorization fits the error tensor well: the training relative errors are small at high ranks, while the test relative errors are small at low ranks.

### 3.4 Tensor Completion

To infer missing entries in the error tensor we collected, namely the entries that take more than the time threshold to evaluate, we use the expectation-maximization (EM) [52], [53] approach together with Tucker decomposition in each step, which we call EM-Tucker and present as Algorithm 7.



**Algorithm 7** EM-Tucker algorithm for tensor completion

---

**Input:** order- $n$  error tensor  $\mathcal{E}$  with missing entries, Tucker ranks  $[r_1, \dots, r_n]$   
**Output:** imputed error tensor  $\mathcal{E}$

- 1  $\mathcal{E}_{\text{obs}} \leftarrow \mathcal{E}$
- 2  $\Omega \leftarrow$  observed entries in  $\mathcal{E}_{\text{obs}}$
- 3 **do**
- 4    $\mathcal{G}, \{U_i\}_{i=1}^n \leftarrow \text{Tucker}(\mathcal{E}, \text{ranks}=[r_1, \dots, r_n])$
- 5    $\mathcal{E}_{\text{pred}} \leftarrow \mathcal{G} \times_1 U_1 \times \dots \times_n U_n$
- 6    $\mathcal{E} \leftarrow \Omega \odot \mathcal{E}_{\text{obs}} + (1 - \Omega) \odot \mathcal{E}_{\text{pred}}$
- 7 **while** not converged

---

In Algorithm 7,  $\Omega$  is similarly a binary tensor that indicates whether each entry of the error tensor  $\mathcal{E}$  is observed or not.  $\Omega$  has the same shape as the original error tensor, with the corresponding entry  $\Omega_{i_1, i_2, \dots, i_n} = 1$  if the  $(i_1, i_2, \dots, i_n)$ -th entry of the error tensor is observed, and 0 otherwise. In our experiments, the algorithm is regarded as converged when the decrease of relative error is less than 0.01%, or the number of iterations reaches 1000.

Why bother with tensor completion? To recover the missing entries of a tensor, we can also perform matrix completion after matricization or perform matrix completion on every slice separately. Tensors are more constrained and so provide better fits to sparse and noisy data. Consider a tensor  $\mathcal{X} \in \mathbb{R}^{I_1 \times I_2 \times \dots \times I_n}$  with Tucker ranks  $[r_1, r_2, \dots, r_n]$ , where  $I_1 = I_2 = \dots = I_n = I$  and  $r_1 = r_2 = \dots = r_n = r$ . The number of degrees of freedom of  $\mathcal{X}$ , which is the minimum number of entries required to recover  $\mathcal{X}$ , is  $r^n + n(rI - r^2) =: m_0$ . If we unfold  $\mathcal{X}$  to  $X \in \mathbb{R}^{I \times I^{n-1}}$ , the number of degrees of freedom of  $X$  is  $(I + I^{n-1} - r)r =: m_1$ . If we treat every slice of  $\mathcal{X}$  separately, the number of degrees of freedom is  $I^{n-2}(2rI - r^2) =: m_2$ . Therefore, when  $r < I$ , we have  $m_0 < m_1 < m_2$ , which means we need fewer parameters to determine  $\mathcal{X}$ , compared to the matricization and union of slices. Thus, tensor completion may outperform matrix completion on  $\mathcal{X}$  with the same number of observed entries.

## 4 KERNEL OBOE

In the offline stage of TENSOROBOE, we used the EM-Tucker algorithm to complete the error tensor we collected. It relies on the assumption that the error tensor has low Tucker rank, which means the embeddings of each pipeline component lie in a low dimensional space. This assumption has been numerically verified in Figure 7. In this section, we turn to the kernel approach that assumes that pipeline embeddings lie in a union of subspaces. We show an efficient kernel method for meta-training that is able to achieve a lower error for tensor completion, and in most cases it gives a better performance for pipeline selection.

KERNEOBOE differs from TENSOROBOE in the tensor completion approach in the offline stage. All the other steps, including the entire online stage, remain the same.

### 4.1 High Rank Matrix Completion for OBOE

Low-rank matrix completion methods are not effective in recovering the missing entries of high-rank matrices even

when the data have some low-dimensional latent structures. As pointed out by Fan et al. [54], data points drawn from each of the following three models can form a high-rank or even full-rank matrix: a union of low-dimensional subspaces, a low-dimensional nonlinear manifolds, and a union of low-dimensional manifolds. Fan et al. [54] showed that, if the columns of a matrix  $M \in \mathbb{R}^{m \times n}$  are generated by  $k$  different polynomials of order at most  $\alpha$  on a  $d$ -dimensional latent variable, the rank of  $M$  can be as high as  $\min\{k \binom{d+\alpha}{\alpha}, m, n\}$ . Thus, when either  $k$  or  $\alpha$  is large,  $M$  can be full-rank. Performing a  $q$ -order polynomial feature map  $\phi$  on each column of  $M$ , they showed that

$$\text{rank}(\phi(M)) \leq \min \left\{ k \binom{d+\alpha q}{\alpha q}, \binom{m+q}{q}, n \right\}. \quad (9)$$

Thus, when  $n$  is sufficiently large and  $d \ll m$ ,  $\phi(M)$  is low-rank, compared to its side lengths. Consequently, the missing entries of  $M$  can be recovered by minimizing the rank (or tractable rank regularizers) of  $\phi(M)$ . The algorithms proposed in [54] require performing SVD on an  $n \times n$  matrix in every iteration and hence are not scalable to very large matrices.

In [55], the authors proposed an efficient high rank matrix completion method called kernelized factorization matrix completion (KFMC). We propose to apply KFMC to the error matrix and solve

$$\begin{aligned} & \text{minimize}_{\hat{E}, D, Z} \frac{1}{2} \|\phi(\hat{E}) - \phi(D)Z\|_F^2 + \frac{\alpha}{2} \|\phi(D)\|_F^2 + \frac{\beta}{2} \|Z\|_F^2 \\ & \text{subject to } \hat{E}_{ij} = E_{ij}, (i, j) \in \Omega, \end{aligned} \quad (10)$$

where  $D \in \mathbb{R}^{m \times r}$ ,  $Z \in \mathbb{R}^{r \times n}$ ,  $r$  denotes the approximate rank of  $\phi(E)$ , and  $\Omega$  consists of the locations of observed entries. Let  $\phi$  be the feature map implicitly determined by the Gaussian RBF kernel  $k(x, y) = \exp(-\|x - y\|_2^2 / (2\sigma^2))$ , then  $\|\phi(D)\|_F^2 \equiv r$ , which means we can remove  $\frac{\alpha}{2} \|\phi(D)\|_F^2$  from (10) without changing the solution. When  $n$  is too large (e.g.  $n \geq 10000$ ), we may use the online algorithm (Algorithm 2) of [55] to solve (10). To further improve efficiency, we extend the online algorithm to a mini-batch algorithm, which is shown in Algorithm 8. In the algorithm,  $\Omega$  consists of the locations of the unknown entries of  $E$ ;  $K_{AB}$  denotes the kernel matrix computed from matrices  $A$  and  $B$ .

Notice the fact that the columns of  $E$  consist of the classification errors given by a few classifiers on the datasets and each classifier may correspond to a low-dimensional subspace of  $\mathbb{R}^m$  or a low-dimensional nonlinear manifold embedded in  $\mathbb{R}^m$ . Therefore, we may model  $E$  more accurately by a high-rank matrix with low-dimensional latent structure. Compared to low-rank matrix completion, KFMC is thus expected to provide higher prediction accuracy of pipeline performance.

### 4.2 Performance Prediction on New Dataset by KFMC

The  $D$  and  $Z$  given by Algorithm 8 can be used to recover the unknown entries of a new column of  $E$  or a new row of  $E$ , which correspond to predicting the performance of a

---

**Algorithm 8** Mini-batch KFMC for Meta-training
 

---

**Input:**  $E_\Omega, r, \sigma, \beta, \eta, n_{\text{batch}}, n_{\text{iter}}, n_{\text{pass}}$

- 1 Initialize:  $D \sim \mathcal{N}(0, 1), \hat{\Delta}_D = 0$
- 2 Split the columns of  $E$  into  $E_1, E_2, \dots, E_{n_{\text{batch}}}$
- 3 **for**  $u = 1$  to  $n_{\text{pass}}$  **do**
- 4     **for**  $j = 1$  to  $n_{\text{batch}}$  **do**
- 5          $l = 0, \hat{\Delta}_{E_j} = 0, C = (K_{DD} + \beta I_r)^{-1}$
- 6         **repeat**
- 7              $l \leftarrow l + 1$  and  $Z_j = CK_{E_j D}^\top$
- 8             Compute  $\Delta_{E_j}$  using (26) of [55]
- 9              $\hat{\Delta}_{E_j} \leftarrow \eta \hat{\Delta}_{E_j} + \Delta_{E_j}$
- 10             $[E_j]_{\Omega_j} \leftarrow [E_j]_{\Omega_j} - [\hat{\Delta}_{E_j}]_{\Omega_j}$
- 11            **until** converged or  $l = n_{\text{iter}}$
- 12            Compute  $\Delta_D$  using (31) of [55]
- 13             $\hat{\Delta}_D \leftarrow \eta \hat{\Delta}_D + \Delta_D$  and  $D \leftarrow D - \hat{\Delta}_D$

**Output:**  $E, D, Z$

---

new pipeline on the existing datasets or the performance of existing pipelines on a new dataset.

To predict the performance of a new pipeline, we can just use the out-of-sample-extension of KFMC, namely the Algorithm 3 of [55]. To predict the performance of the pipelines on a new dataset, we may need to solve the following problem

$$\begin{aligned} & \underset{\hat{E}', D'}{\text{minimize}} \quad \frac{1}{2} \|\phi(\hat{E}') - \phi(D')Z\|_{\mathbb{F}}^2 & (11) \\ & \text{subject to} \quad \hat{E}'_{ij} = E'_{ij}, (i, j) \in \Omega', \end{aligned}$$

where  $E' = \begin{bmatrix} E \\ e_{\text{new}} \end{bmatrix}$ ,  $D' = \begin{bmatrix} D \\ d_{\text{new}} \end{bmatrix}$ ,  $\Omega' = \Omega \cup \omega_{\text{new}}$ , and  $\omega_{\text{new}}$  denotes the locations of known entries of  $e_{\text{new}}$ . Obviously, solving (11) is time-consuming, even when we fix  $E$  and  $D$ .

We can write  $\phi(x) = c \begin{bmatrix} x \\ \tilde{\phi}(x) \end{bmatrix}$ , where  $\tilde{\phi}$  consists of the features of  $\phi$  with  $x$  itself removed and  $c$  is a constant. Then we have

$$\phi(E') = \phi(D')Z \implies E' = D'Z.$$

Therefore we propose to solve

$$\begin{aligned} & \underset{\hat{e}_{\text{new}}, d_{\text{new}}}{\text{minimize}} \quad \frac{1}{2} \|\hat{e}_{\text{new}} - d_{\text{new}}Z\|^2 + \frac{\alpha}{2} \|d_{\text{new}}\|^2 & (12) \\ & \text{subject to} \quad \hat{e}_j = e_j, j \in \omega. \end{aligned}$$

Compared to Problem 11, Problem 12 drops the higher order terms from objective function and has the advantage of a closed-form solution  $[\hat{e}_{\text{new}}]_{\tilde{\omega}} = d_{\text{new}}Z_{:, \tilde{\omega}}$ , where  $d_{\text{new}} = e_\omega Z_{:, \omega}^\top (Z_{:, \omega} Z_{:, \omega}^\top + \alpha I_r)^{-1}$ .

### 4.3 Experimental Design with KFMC

Since the prediction model used in (12) is similar to (1), the experimental design of KFMC can be easily adapted from Section 2.4.

## 5 EXPERIMENTS

All the code is in the GitHub repository at <https://github.com/udellgroup/oboe>. We use Intel<sup>®</sup> Xeon<sup>®</sup> E7-4850 v4

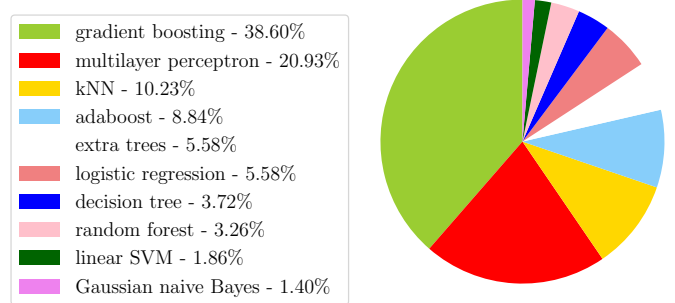


Figure 9: Which estimators work best? Distribution of estimator types in best pipelines on meta-training datasets.

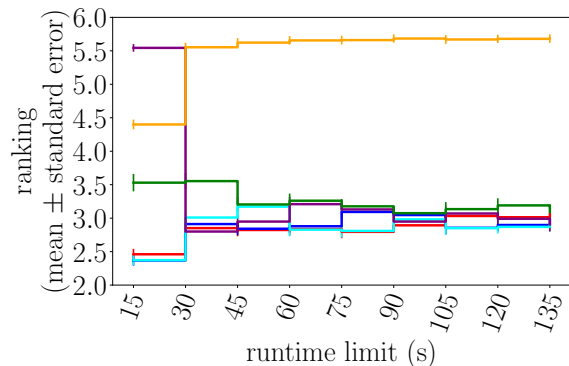
2.10GHz CPUs for evaluation. Offline, we collect cross-validated pipeline performance on meta-training datasets: 215 OpenML [56], [57] classification datasets with number of data points between 150 and 10,000, chosen alphabetically, and listed in Appendix A.1. In TENSOROBOE and KERNELOBOE, pipelines are combinations of the machine learning components shown in Appendix A.3, Table 2, which lists 4 data imputers, 2 encoders, 2 standardizers, 8 dimensionality reducers and 183 estimators. Here we have 23,424 possible pipeline combinations in total, but we are demonstrating the ability of our methods to quickly explore the combinatorial space. Because of ensembling, our methods are able to handle a much larger number of combinations. In OBOE, we only vary estimators among the above 183, after preprocessing all datasets by imputing with mean (for numerical features) or mode (categorical features), one-hot encoding categorical features and then standardizing all features to have zero mean and unit variance. Thus the search space of OBOE is a slice of those in TENSOROBOE and KERNELOBOE.

### 5.1 Comparison of Time-Constrained AutoML Systems

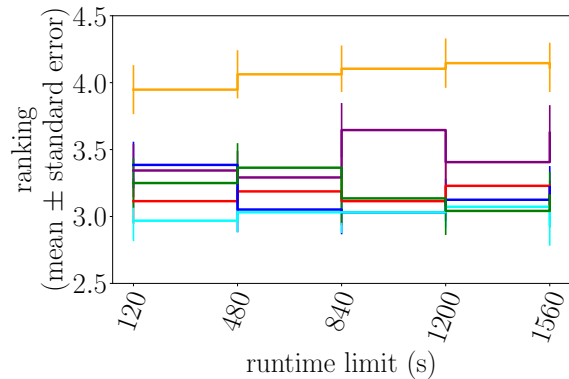
In this section, we demonstrate the performance of OBOE and TENSOROBOE as AutoML systems. A naive approach for pipeline selection is to choose the one that on average performs the best among all meta-training datasets, which we call the baseline pipeline. Given the pipeline selection problem, it is common for human practitioners to try out the best pipeline at the very beginning. On our meta-training datasets, the baseline pipeline is: impute missing entries with the mode, encode categorical features as integers, standardize each feature, remove features with 0 variance, and classify by gradient boosting with learning rate 0.25 and maximum depth 3. The baseline pipeline has an average ranking of 1568 among all 23,424 pipelines across all 215 meta-training datasets.

Human practitioners may also reduce the number of trials by choosing certain pipeline components to be the type that performs the best on average. Figure 9, however, shows that although some estimator types (gradient boosting and multilayer perceptron) are commonly seen among the best pipelines, no estimator type uniformly dominates the rest.

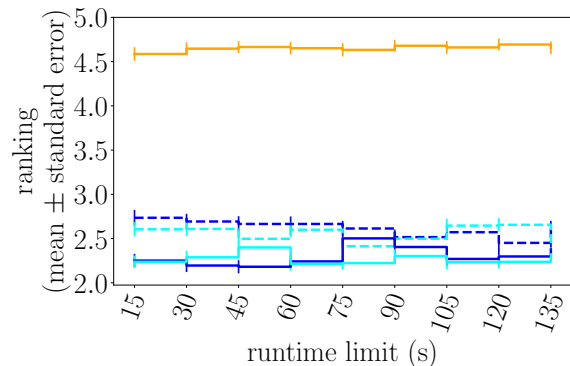
In the first experiment, we compare OBOE, TENSOROBOE and KERNELOBOE that work on the original error matrix and error tensor with auto-sklearn [3], TPOT [2], and



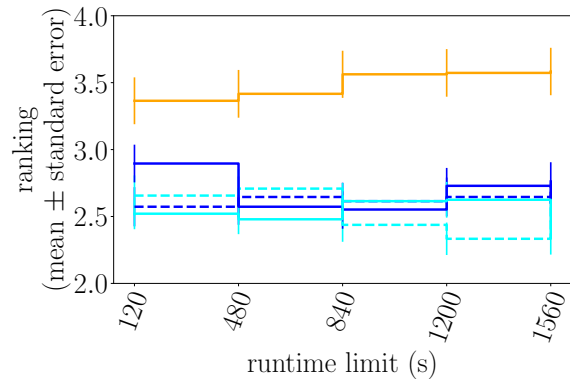
(a) OpenML (meta-LOOCV)



(b) UCI (meta-test)



(a) OpenML (meta-LOOCV)



(b) UCI (meta-test)



Figure 10: System rankings of AutoML systems for pipeline search in a time-constrained setting, vs the baseline pipeline. We meta-train on OpenML classification datasets and meta-test on UCI classification datasets [58]. Until the first time the system can produce a pipeline, we classify every data point with the most common class label. Lower ranks are better.

the baseline pipeline. To ensure fair comparisons, we use a single CPU core for each AutoML system. We allow each to choose from the same primitives. The comparison plot is shown as Figure 10. We can see that:

- 1 All AutoML frameworks are able to construct pipelines that outperform the baseline on average once the method returns a pipeline (for auto-sklearn, this takes 30 seconds).
- 2 The OBOE variants on average outperform the competing methods and produces meaningful pipeline configurations fastest.
- 3 With much longer running time on meta-test datasets, shown in Figure 10b, our OBOE and TENSOROBOE still outperforms in most cases. This shows that they are able to approximate the hyperparameter landscape accurately in general, which will be discussed to greater detail in Section 5.5.

In the second experiment, we compare the performance of TENSOROBOE and KERNELOBOE that take randomly subsampled error tensors as input, and show the result in Figure 11. Offline, given the collected error tensor  $\mathcal{E}$  with

Figure 11: System rankings of TENSOROBOE and KERNELOBOE for pipeline search with randomly subsampled error tensors, vs the baseline pipeline. The error tensor used by the dashed lines marked as “subsampled, random” lacks 90% of the pipeline performance that were known in the original tensor. Dataset and estimator ranks are set to be 40 to complete the error tensor in TENSOROBOE.

missing ratio 3.3%, we randomly subsample 10% of its known entries and regard the rest as missing, resulting in a missing ratio of 90.3%. We denote this tensor as  $\mathcal{E}_\Omega$ . We then use Algorithm 7 and Algorithm 8, respectively, to complete  $\mathcal{E}_\Omega$ , and use the respective results as the error tensor for TENSOROBOE and KERNELOBOE. We can see that:

- 1 Results from the subsampled error tensor are in general worse than those from the original error tensor at smaller running times, indicating the abundance of meta-training data does help in the scarcity of computational power.
- 2 Results from the subsampled error tensor have higher rankings (corresponding to smaller ranking values) at longer runtime thresholds, indicating that the meta-testing process gains more knowledge of the pipeline performance space with more time. This opens up the horizon of a meta-training process that collects pipeline performance data on a larger space with more model types for each of the pipeline components.

In the third experiment, we compare the performance

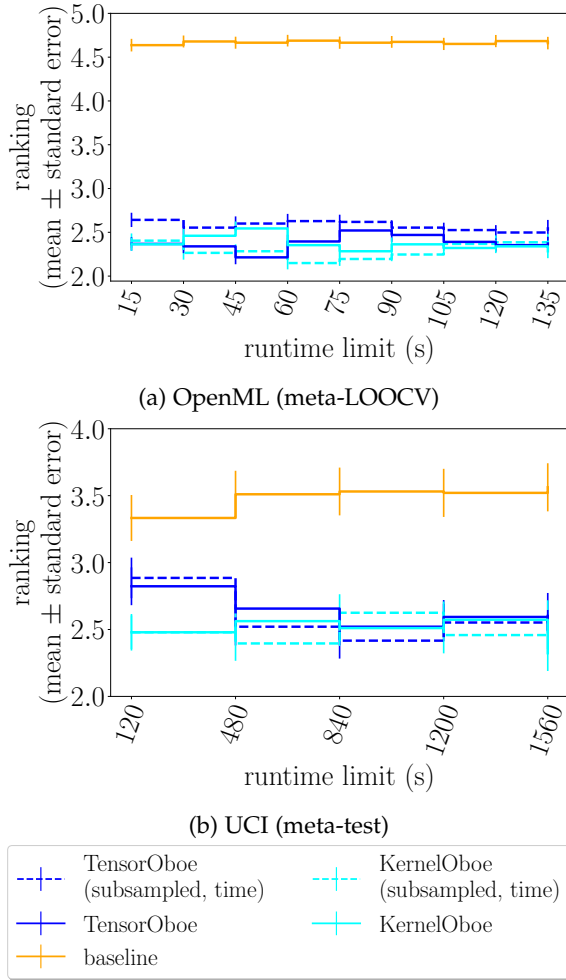


Figure 12: System rankings of TENSOROBOE and KERNELOBOE for pipeline search with time-thresholded error tensors, vs the baseline pipeline. The error tensor used by the dashed lines marked as “subsampled, time” lacks all pipeline performance that take more than 20 seconds to evaluate. Dataset and estimator ranks are set to be 25 to complete the error tensor in TENSOROBOE.

of TENSOROBOE and KERNELOBOE with the error tensor that only contain pipeline execution results that take less than 20 seconds. This error tensor has 9.2% entries missing, compared to the original 3.3% missing ratio with the time threshold of 120 seconds. Same as the evaluation above, we compare the performance of TENSOROBOE and KERNELOBOE as AutoML systems and show the results in Figure 12. We can see similar trends as above.

## 5.2 Comparison of Completion Methods

In this section, we compare the performance of EM algorithm on matrix and tensor completion, and KFMC on our error tensor. We explore two completion scenarios: entries missing at random, and entries with a longer running time missing.

### 5.2.1 Uniformly Sample the Error Tensor

Given meta-training data  $\{\mathcal{D}, \mathcal{P}, \mathcal{P}(\mathcal{D})\}$  on a subset of dataset-pipeline combinations, a good surrogate model

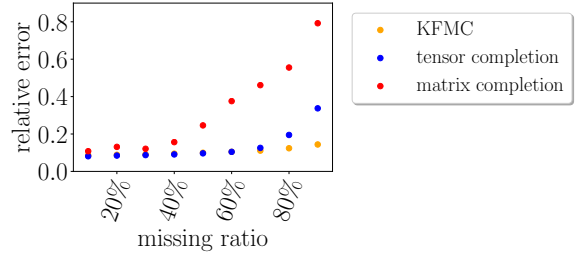


Figure 13: Prediction performance on pipeline-dataset combinations that are missing at random. Dataset and estimator ranks for tensor and matrix completions are set to be 40. The  $r$  in KFMC is set to be 215.

should be able to accurately predict the performance of new dataset-pipeline combinations.

We explore the setting commonly seen in matrix completion literature: entries are missing at random with a given missing ratio. Practitioners may thus subsample pipeline-dataset combinations in the meta-training phase to reduce the number of evaluations.

Figure 13 shows the relative error on entries that are taken out at random. To ensure a fair comparison, we set the dataset and estimator ranks to be equal in the tensor model, which is required for the matrix model, since column rank equals row rank for a matrix. We can see that:

- 1 The tensor model outperforms matrix in all cases, demonstrating that the additional combinatorial structure provided by the tensor model helps us recover the combinatorial relationships among different pipeline components.
- 2 KFMC achieves lower error on all missing ratio settings and has no drastic increase in relative error in almost the entire range of missing ratios, making it possible for drastic subsampling to save computing power in meta-training.

### 5.2.2 Sample the Error Tensor by Running Time

In this scenario, we explore the effect of only collecting fastest pipeline-dataset combinations in meta-learning. Figure 14 shows that most pipelines run quickly on most datasets: for example, over 90% finish in less than 20 seconds and over 95% finish in less than 80 seconds.

Figure 15 compares relative errors of predictions by tensor and matrix surrogate models. For each runtime threshold, we treat pipeline-dataset combinations with running time less than the threshold as training data, and those with running time longer than threshold and less than 120 seconds as test data. We compute relative errors on test data, hence the name “runtime generalization”. In addition to the observation in Section 5.2.1 on the advantage of tensor completion versus matrix completion, we can see from Figure 15b, the U-shaped curve of relative error when increasing dataset and estimator ranks for both matrix and tensor model, that the low rank models change from underfitting to overfitting as the ranks increase. Thus we select both dataset and estimator ranks to be 20, the rank in the middle, in TENSOROBOE.

Figure 16 shows the relative error on entries that are missing by runtime thresholding, which are the entries with runtime between the corresponding threshold and the

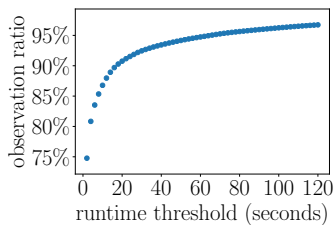


Figure 14: CDF of pipeline runtime on meta-training datasets.

runtime upper limit in error tensor collect (120 seconds in our experiments). Similar to Section 5.2.1, we can see that:

- 1 Tensor completion has smaller error than matrix completion in almost all cases.
- 2 Relative to the EM approach for tensor and matrix completions, KFMC outperforms at smaller runtime thresholds, which is more interesting in practice.

### 5.3 Pipeline Selection by Greedy Experiment Design

We compare the performance of different approaches to solve the experiment design problem, so as to choose which pipelines we should sample.

Recall that there are two approaches:

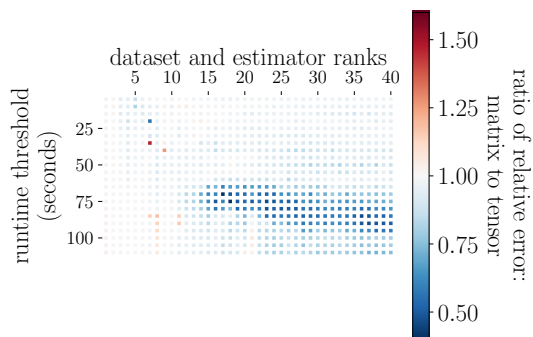
- **Convexification:** Solve the relaxed problem (Equation 6 with  $v_i \in [0, 1], \forall i \in [n]$ ) with an SLSQP solver, sort the entries in the optimal solution  $v^*$ , and greedily add the pipeline with large  $v_i^*$ , until the runtime limit is reached.
- **Greedy:** Solve the original integer programming problem (Equation 6) by the greedy algorithm (Algorithm 5), initialized by time-constrained QR (Algorithm 6).

For our problem, the greedy approach is superior, since the convexification method is prohibitive on our large 215-by-23424 error matrix. Hence we compare these methods on a subset of pipelines that only differ by estimators, 183 in total. This is the same as the setting in Oboe [12]. Shown in Figure 17, we can see that:

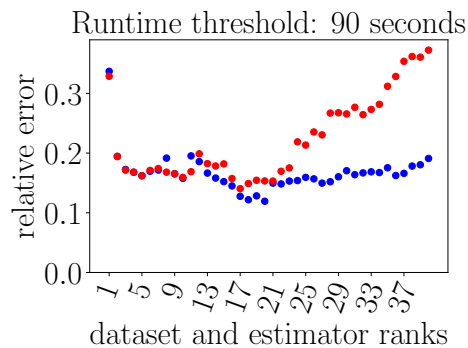
- 1 The greedy method performs better for cold-start than convexification (Figure 17a): it selects informative designs that better predict the high-percentage pipelines when selecting similar number of designs (Figure 17b).
- 2 The greedy method is more than  $30\times$  faster than convexification, which allows the AutoML system to devote its runtime budget to fitting pipelines instead of searching for the informative pipelines.
- 3 Shown in Figure 17d, the greedy algorithm would still take a fair amount of time if the number of designs we select is large; however, the dataset ranks we choose are less than 50, which means it generally takes less than 10 seconds to choose informative pipelines.

### 5.4 Pipeline Runtime Prediction Performance

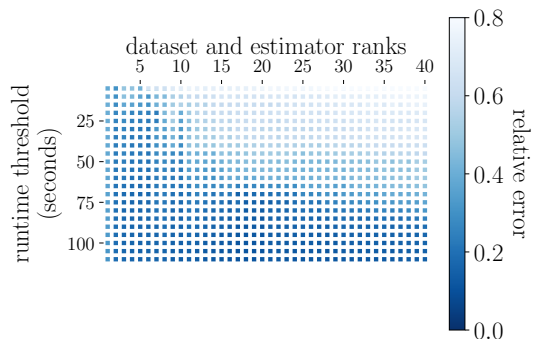
The extent of how accurate we can predict running times of pipelines greatly affects performance of our time-constrained pipeline selection system. Recall that we use order-3 polynomial regression on  $n^{\mathcal{D}}$  and  $p^{\mathcal{D}}$ , the numbers of data points and features in  $\mathcal{D}$ , and their logarithms. We



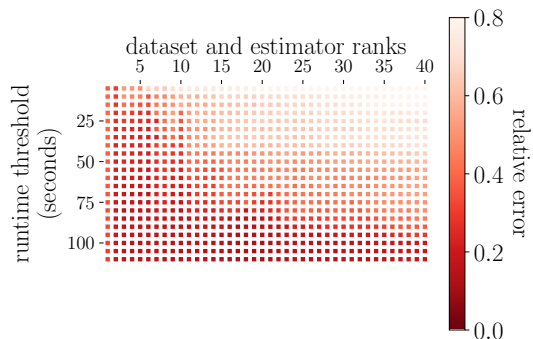
(a) Runtime generalization by tensor vs matrix models. Blue denotes that the tensor model is better in achieving a smaller error for pipeline evaluations with longer running time. Red denotes the matrix model is better.



(b) An example of tensor completion and matrix completion errors with runtime threshold to be 90 seconds for pipeline performance collection. Error tensor missing ratio 3.3%.



(c) Runtime generalization error by tensor model. Darker the color, smaller the error.



(d) Runtime generalization error by matrix model. Darker the color, smaller the error.



Figure 15: Tensor completion vs matrix completion for inferring pipeline performance.

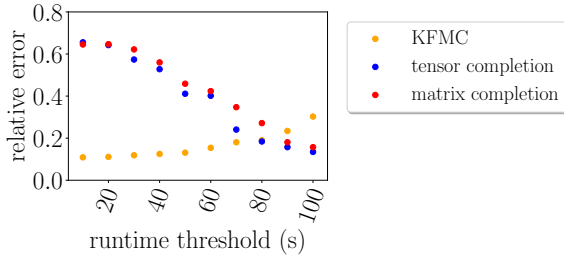


Figure 16: Prediction results on pipeline-dataset combinations that are missing by runtime thresholding: results of combinations that take longer than the threshold are missing. Dataset and estimator ranks for tensor and matrix completions are set to be 25. The  $r$  in KPMC is set to be 215.

Table 1: Runtime prediction accuracy on OpenML datasets

Pipeline estimator type	Runtime prediction accuracy	
	within factor of 2	within factor of 4
Adaboost	73.6%	86.9%
Decision tree	62.7%	78.9%
Extra trees	71.0%	83.8%
Gradient boosting	53.4%	77.5%
Gaussian naive Bayes	67.3%	82.3%
kNN	68.7%	84.4%
Logistic regression	53.6%	76.1%
Multilayer perceptron	74.5%	88.9%
Perceptron	64.5%	82.2%
Random Forest	69.5%	84.9%
Linear SVM	56.8%	79.5%

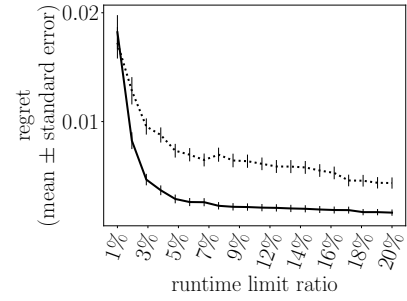
shown in Table 1 that this runtime predictor performs well. Visualization plots that previously appeared in [12] is in Appendix E, Figure 22.

## 5.5 Learning the Hyperparameter Landscapes

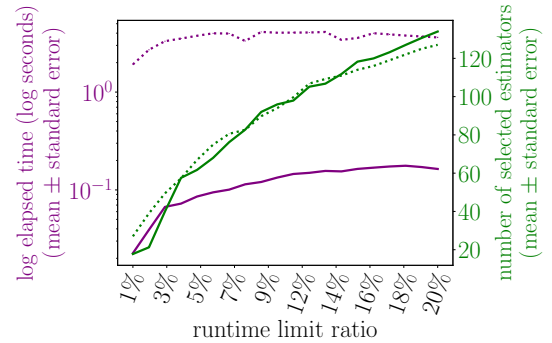
Hyperparameter landscapes plot pipeline performance with respect to hyperparameter values. While parameter landscapes have been extensively studied, especially in the deep learning context (for example, [59], [60], [61]), hyperparameter landscapes are less studied. The previous sections focus on how we can choose among different pipeline component types. In this section, we show that our tensor surrogate model is able to learn hyperparameter landscapes of different estimator types that exhibit qualitatively different behaviors.

Figure 18 shows some examples of both real and predicted hyperparameter landscapes after running our system for 135 seconds. We can see that our predictions match the overall tendencies of the curves. Their zoomed-in version, shown as Appendix D, Figure 21, show that our predictions can also capture most of the small variations in these landscapes.

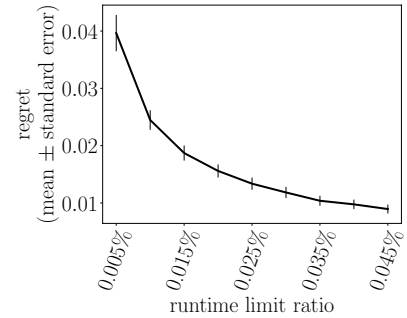
Note our methods do not include a subroutine for hyperparameter optimization: it sets a grid of hyperparameter values for each estimator, instead of optimizing hyperparameters by, for example, Bayesian optimization. We show by some hyperparameter landscapes that our grid search effectively sample performant hyperparameter settings within the range of hyperparameters, thus a coarse grid suffices.



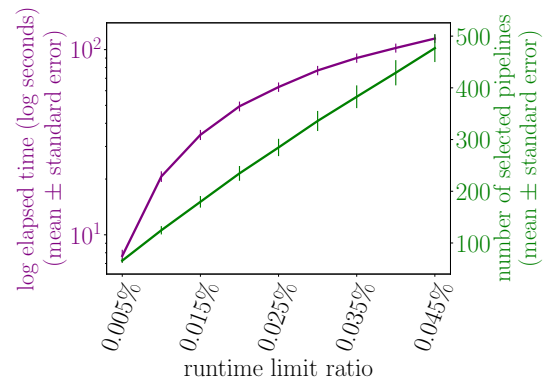
(a) Regret on the subsampled error matrix (215-by-183) for estimator search.



(b) Experiment design running time and number of selected estimators on the subsampled error matrix for estimator search.



(c) Regret on the full error matrix (215-by-23424) for pipeline search, by the greedy method.



(d) Experiment design running time and number of selected pipelines on the full error matrix for pipeline search, by the greedy method.

⋯ convexification    —+ greedy

Figure 17: Time-constrained experiment design methods across meta-training datasets. The y-axes in 17a and 17c are regrets: the difference between minimum pipeline error found by the respective approaches and the actual one. The x-axes are runtime limit ratios: ratios of the runtime limit to the total running time of all pipelines on each dataset.

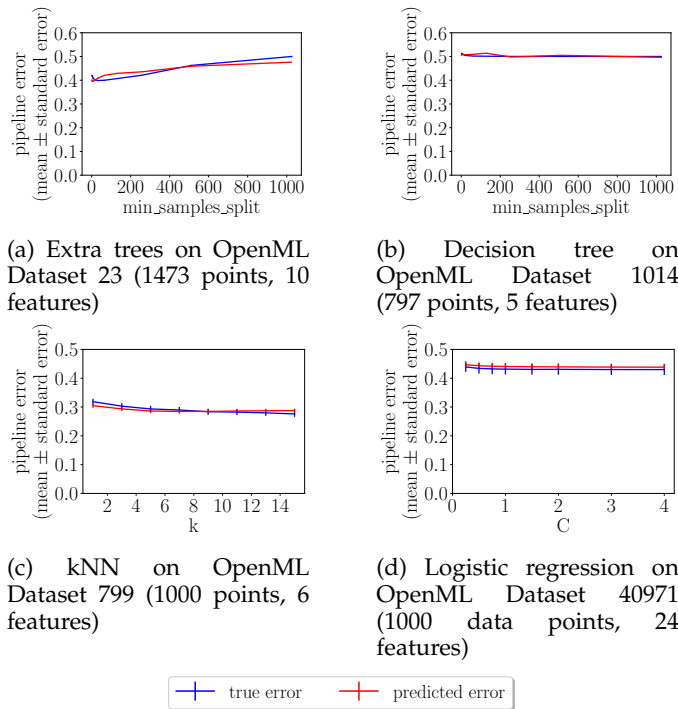


Figure 18: Hyperparameter landscape prediction examples.

## 6 CONCLUSION

This paper develops structured models for AutoML pipeline selection. The low rank matrix, low Tucker rank tensor and kernelized matrix surrogate model allows us to efficiently learn about new datasets. Also, we design greedy experiment design methods to select informative pipelines to evaluate. Empirically, this method improves on the state of the art in AutoML pipeline selection.

There are many avenues for improvement and extensions. For example, one could enlarge the pipeline search space, explore different mechanisms to initialize the greedy method, develop an extension for neural architecture search, and design task-oriented pipeline selection systems that have better performance on domain-specific datasets.

## ACKNOWLEDGMENTS

This work was supported in part by DARPA Award FA8750-17-2-0101. The authors thank Christophe Giraud-Carrier, Ameet Talwalkar, Iddo Drori, Thorsten Joachims, Raul Astudillo Marban, Matthew Zalesak, Lijun Ding and Davis Wertheimer for helpful discussions, and thank Jack Dunn for a script to parse UCI Machine Learning Repository datasets.

## REFERENCES

- [1] D. H. Wolpert and W. G. Macready, "No free lunch theorems for optimization," *IEEE transactions on evolutionary computation*, vol. 1, no. 1, pp. 67–82, 1997.
- [2] R. S. Olson and J. H. Moore, "Tpot: A tree-based pipeline optimization tool for automating machine learning," in *Automated Machine Learning*. Springer, 2019, pp. 151–160.
- [3] M. Feurer, A. Klein, K. Eggenberger, J. Springenberg, M. Blum, and F. Hutter, "Efficient and robust automated machine learning," in *Advances in neural information processing systems*, 2015, pp. 2962–2970.
- [4] I. Drori, Y. Krishnamurthy, R. Rampin, R. Lourenço, J. One, K. Cho, C. Silva, and J. Freire, "Alphad3m: Machine learning pipeline synthesis," in *AutoML Workshop at ICML*, 2018.
- [5] S. Liu, P. Ram, D. Vijaykeerthy, D. Bouneffouf, G. Bramble, H. Samulowitz, D. Wang, A. Conn, and A. Gray, "An admm based framework for automl pipeline configuration," *arXiv preprint arXiv:1905.00424*, 2019.
- [6] G. E. Box, "Science and statistics," *Journal of the American Statistical Association*, vol. 71, no. 356, pp. 791–799, 1976.
- [7] S. Thrun and L. Pratt, *Learning to learn*. Springer Science & Business Media, 2012.
- [8] M. Andrychowicz, M. Denil, S. Gomez, M. W. Hoffman, D. Pfau, T. Schaul, B. Shillingford, and N. De Freitas, "Learning to learn by gradient descent by gradient descent," in *Advances in neural information processing systems*, 2016, pp. 3981–3989.
- [9] B. M. Lake, T. D. Ullman, J. B. Tenenbaum, and S. J. Gershman, "Building machines that learn and think like people," *Behavioral and brain sciences*, vol. 40, 2017.
- [10] J. Vanschoren, "Meta-learning: A survey," *arXiv preprint arXiv:1810.03548*, 2018.
- [11] Z. Shang, E. Zraggen, B. Buratti, F. Kossmann, P. Eichmann, Y. Chung, C. Binnig, E. Upfal, and T. Kraska, "Democratizing data science through interactive curation of ml pipelines," in *Proceedings of the 2019 International Conference on Management of Data*, 2019, pp. 1171–1188.
- [12] C. Yang, Y. Akimoto, D. W. Kim, and M. Udell, "Oboe: Collaborative filtering for automl model selection," in *Proceedings of the 25th ACM SIGKDD International Conference on Knowledge Discovery & Data Mining*, 2019, pp. 1173–1183.
- [13] B. Pfahringer, H. Bensusan, and C. G. Giraud-Carrier, "Meta-Learning by Landmarking Various Learning Algorithms," in *ICML*, 2000, pp. 743–750.
- [14] M. Feurer, J. T. Springenberg, and F. Hutter, "Using meta-learning to initialize Bayesian optimization of hyperparameters," in *International Conference on Meta-learning and Algorithm Selection*. Citeseer, 2014, pp. 3–10.
- [15] N. Fusi, R. Sheth, and M. Elibol, "Probabilistic matrix factorization for automated machine learning," in *Advances in Neural Information Processing Systems*, 2018, pp. 3352–3361.
- [16] M. Wistuba, N. Schilling, and L. Schmidt-Thieme, "Learning hyperparameter optimization initializations," in *IEEE International Conference on Data Science and Advanced Analytics*, Oct 2015, pp. 1–10.
- [17] I. Drori, L. Liu, Y. Nian, S. C. Koorathota, J. S. Li, A. K. Moretti, J. Freire, and M. Udell, "Automl using metadata language embeddings," *arXiv preprint arXiv:1910.03698*, 2019.
- [18] C. E. Rasmussen and C. K. Williams, *Gaussian processes for machine learning*. the MIT Press, 2006.
- [19] J. Snoek, H. Larochelle, and R. P. Adams, "Practical Bayesian optimization of machine learning algorithms," in *Advances in Neural Information Processing Systems*, 2012, pp. 2951–2959.
- [20] J. S. Bergstra, R. Bardenet, Y. Bengio, and B. Kégl, "Algorithms for hyper-parameter optimization," in *Advances in Neural Information Processing Systems*, 2011, pp. 2546–2554.
- [21] P. Sebastiani and H. P. Wynn, "Maximum entropy sampling and optimal Bayesian experimental design," *Journal of the Royal Statistical Society: Series B (Statistical Methodology)*, vol. 62, no. 1, pp. 145–157, 2000.
- [22] R. Herbrich, N. D. Lawrence, and M. Seeger, "Fast sparse Gaussian process methods: The informative vector machine," in *Advances in Neural Information Processing Systems*, 2003, pp. 625–632.
- [23] D. J. MacKay, "Information-based objective functions for active data selection," *Neural Computation*, vol. 4, no. 4, pp. 590–604, 1992.
- [24] N. Srinivas, A. Krause, S. Kakade, and M. Seeger, "Gaussian Process Optimization in the Bandit Setting: No Regret and Experimental Design," in *ICML*, 2010, pp. 1015–1022.
- [25] E. Hazan, A. Klivans, and Y. Yuan, "Hyperparameter optimization: a spectral approach," in *ICLR*, 2018. [Online]. Available: <https://openreview.net/forum?id=H1zriGeCZ>
- [26] T. Bartz-Beielstein and S. Markon, "Tuning search algorithms for real-world applications: A regression tree based approach," in *Congress on Evolutionary Computation*, vol. 1. IEEE, 2004, pp. 1111–1118.
- [27] F. Hutter, H. H. Hoos, and K. Leyton-Brown, "Sequential Model-Based Optimization for General Algorithm Configuration." *LION*, vol. 5, pp. 507–523, 2011.

- [28] A. Wald, "On the efficient design of statistical investigations," *The Annals of Mathematical Statistics*, vol. 14, no. 2, pp. 134–140, 1943.
- [29] R. S. John and N. R. Draper, "D-optimality for regression designs: a review," *Technometrics*, vol. 17, no. 1, pp. 15–23, 1975.
- [30] F. Pukelsheim, *Optimal design of experiments*. SIAM, 1993, vol. 50.
- [31] S. Boyd and L. Vandenberghe, *Convex optimization*. Cambridge University Press, 2004.
- [32] V. Madan, M. Singh, U. Tantipongpipat, and W. Xie, "Combinatorial algorithms for optimal design," in *Conference on Learning Theory*, 2019, pp. 2210–2258.
- [33] T. G. Kolda and B. W. Bader, "Tensor decompositions and applications," *SIAM review*, vol. 51, no. 3, pp. 455–500, 2009.
- [34] T. G. Dietterich, "Ensemble methods in machine learning," in *International workshop on multiple classifier systems*. Springer, 2000, pp. 1–15.
- [35] L. Breiman, "Bagging predictors," *Machine learning*, vol. 24, no. 2, pp. 123–140, 1996.
- [36] R. E. Schapire, "The boosting approach to machine learning: An overview," in *Nonlinear estimation and classification*. Springer, 2003, pp. 149–171.
- [37] D. H. Wolpert, "Stacked generalization," *Neural networks*, vol. 5, no. 2, pp. 241–259, 1992.
- [38] G. H. Golub and C. F. Van Loan, *Matrix computations*. JHU press, 2012, vol. 3.
- [39] G. L. Nemhauser, L. A. Wolsey, and M. L. Fisher, "An analysis of approximations for maximizing submodular set functions," *Mathematical programming*, vol. 14, no. 1, pp. 265–294, 1978.
- [40] D. Sharma, A. Kapoor, and A. Deshpande, "On greedy maximization of entropy," in *International Conference on Machine Learning*, 2015, pp. 1330–1338.
- [41] A. Krause, A. Singh, and C. Guestrin, "Near-optimal sensor placements in gaussian processes: Theory, efficient algorithms and empirical studies," *Journal of Machine Learning Research*, vol. 9, no. Feb, pp. 235–284, 2008.
- [42] A. Krause and D. Golovin, "Submodular function maximization." 2014.
- [43] D. A. Harville, "Matrix algebra from a statistician's perspective," 1998.
- [44] J. Sherman and W. J. Morrison, "Adjustment of an inverse matrix corresponding to a change in one element of a given matrix," *The Annals of Mathematical Statistics*, vol. 21, no. 1, pp. 124–127, 1950.
- [45] W. W. Hager, "Updating the inverse of a matrix," *SIAM review*, vol. 31, no. 2, pp. 221–239, 1989.
- [46] M. Gu and S. C. Eisenstat, "Efficient algorithms for computing a strong rank-revealing qr factorization," *SIAM Journal on Scientific Computing*, vol. 17, no. 4, pp. 848–869, 1996.
- [47] F. Hutter, L. Xu, H. H. Hoos, and K. Leyton-Brown, "Algorithm runtime prediction: Methods & evaluation," *Artificial Intelligence*, vol. 206, pp. 79–111, 2014.
- [48] J. D. Carroll and J.-J. Chang, "Analysis of individual differences in multidimensional scaling via an n-way generalization of "eckart-young" decomposition," *Psychometrika*, vol. 35, no. 3, pp. 283–319, 1970.
- [49] R. A. Harshman *et al.*, "Foundations of the parafac procedure: Models and conditions for an "explanatory" multimodal factor analysis," 1970.
- [50] L. R. Tucker, "Some mathematical notes on three-mode factor analysis," *Psychometrika*, vol. 31, no. 3, pp. 279–311, 1966.
- [51] I. V. Oseledets, "Tensor-train decomposition," *SIAM Journal on Scientific Computing*, vol. 33, no. 5, pp. 2295–2317, 2011.
- [52] A. P. Dempster, N. M. Laird, and D. B. Rubin, "Maximum likelihood from incomplete data via the em algorithm," *Journal of the Royal Statistical Society: Series B (Methodological)*, vol. 39, no. 1, pp. 1–22, 1977.
- [53] Q. Song, H. Ge, J. Caverlee, and X. Hu, "Tensor completion algorithms in big data analytics," *ACM Transactions on Knowledge Discovery from Data (TKDD)*, vol. 13, no. 1, pp. 1–48, 2019.
- [54] J. Fan, Y. Zhang, and M. Udell, "Polynomial matrix completion for missing data imputation and transductive learning," *arXiv preprint arXiv:1912.06989*, 2019.
- [55] J. Fan and M. Udell, "Online high rank matrix completion," in *Proceedings of the IEEE Conference on Computer Vision and Pattern Recognition*, 2019, pp. 8690–8698.
- [56] J. Vanschoren, J. N. van Rijn, B. Bischl, and L. Torgo, "Openml: Networked science in machine learning," *SIGKDD Explorations*, vol. 15, no. 2, pp. 49–60, 2013. [Online]. Available: <http://doi.acm.org/10.1145/2641190.2641198>
- [57] A. K. P. G. N. M. S. R. A. M. J. V. F. H. Matthias Feurer, Jan N. van Rijn, "Openml-python: an extensible python api for openml," *arXiv*, vol. 1911.02490. [Online]. Available: <https://arxiv.org/pdf/1911.02490.pdf>
- [58] D. Dua and C. Graff, "UCI machine learning repository," 2017. [Online]. Available: <http://archive.ics.uci.edu/ml>
- [59] N. S. Keskar, D. Mudigere, J. Nocedal, M. Smelyanskiy, and P. T. P. Tang, "On large-batch training for deep learning: Generalization gap and sharp minima," 2017.
- [60] H. Li, Z. Xu, G. Taylor, C. Studer, and T. Goldstein, "Visualizing the loss landscape of neural nets," in *Advances in Neural Information Processing Systems*, 2018, pp. 6389–6399.
- [61] T. Garipov, P. Izmailov, D. Podoprikin, D. P. Vetrov, and A. G. Wilson, "Loss surfaces, mode connectivity, and fast ensembling of dnns," in *Advances in Neural Information Processing Systems*, 2018, pp. 8789–8798.
- [62] F. Pedregosa, G. Varoquaux, A. Gramfort, V. Michel, B. Thirion, O. Grisel, M. Blondel, P. Prettenhofer, R. Weiss, V. Dubourg, J. Vanderplas, A. Passos, D. Cournapeau, M. Brucher, M. Perrot, and E. Duchesnay, "Scikit-learn: Machine learning in Python," *Journal of Machine Learning Research*, vol. 12, pp. 2825–2830, 2011.

**Chengrun Yang** received his BS degree in Physics from Fudan University, Shanghai, China in 2016. Currently, he is a PhD student at the School of Electrical and Computer Engineering, Cornell University. His research interests include the application of low dimensional structures and active learning in resource-constrained learning problems.

**Jicong Fan** received his BE and ME degrees in Automation and Control Science & Engineering, from Beijing University of Chemical Technology, Beijing, China, in 2010 and 2013, respectively. From 2013 to 2015, he was a research assistant at the University of Hong Kong. He received his PhD degree in Electronic Engineering, from City University of Hong Kong, Hong Kong S.A.R. in 2018. From 2018.01 to 2018.06, he was a visiting scholar at the Department of Electrical and Computer Engineering, University of Wisconsin-Madison, USA. Currently, he is a postdoc associate at the School of Operations Research and Information Engineering, Cornell University, Ithaca, USA. His research interests include computer vision, machine learning, and optimization.

**Ziyang Wu** received the BS degree from Cornell University in 2019. He is currently a Masters student in Computer Science at Cornell University. His research interests include computer vision and meta learning, especially in automated machine learning.

**Madeleine Udell** is Assistant Professor of Operations Research and Information Engineering and Richard and Sybil Smith Sesquicentennial Fellow at Cornell University. She studies optimization and machine learning for large scale data analysis and control, with applications in marketing, demographic modeling, medical informatics, engineering system design, and automated machine learning. Her work has been recognized by an NSF CAREER award, an Office of Naval Research (ONR) Young Investigator Award, and an INFORMS Optimization Society Best Student Paper Award (as advisor). Madeleine completed her PhD at Stanford University in Computational & Mathematical Engineering in 2015 under the supervision of Stephen Boyd, and a one year postdoctoral fellowship at Caltech in the Center for the Mathematics of Information hosted by Professor Joel Tropp.



## APPENDIX A DATASET AND PIPELINE CONFIGURATIONS

### A.1 Meta-training OpenML Datasets

Indices of the OpenML datasets we use for meta-training: 2, 3, 5, 7, 9, 11, 12, 13, 14, 15, 16, 18, 20, 22, 23, 24, 25, 27, 28, 29, 30, 31, 35, 36, 37, 38, 39, 40, 41, 42, 44, 46, 48, 50, 53, 54, 59, 60, 181, 182, 183, 187, 285, 307, 313, 316, 329, 336, 337, 338, 375, 377, 389, 446, 450, 458, 463, 469, 475, 694, 715, 717, 718, 720, 721, 723, 725, 728, 730, 732, 733, 735, 737, 740, 742, 743, 744, 745, 746, 747, 748, 749, 750, 751, 753, 763, 769, 773, 776, 778, 779, 788, 792, 794, 796, 797, 799, 803, 805, 806, 807, 813, 818, 819, 820, 824, 825, 826, 830, 832, 837, 838, 847, 853, 855, 863, 866, 869, 870, 871, 873, 877, 880, 884, 888, 896, 900, 903, 904, 906, 907, 908, 909, 910, 911, 912, 913, 915, 917, 920, 923, 925, 926, 933, 934, 935, 936, 937, 941, 943, 952, 953, 954, 955, 958, 962, 970, 971, 973, 976, 978, 979, 980, 983, 987, 991, 994, 995, 996, 997, 1005, 1011, 1012, 1014, 1016, 1020, 1021, 1022, 1025, 1026, 1038, 1039, 1041, 1042, 1048, 1049, 1050, 1054, 1056, 1063, 1065, 1067, 1068, 1069, 1071, 1073, 1100, 1115, 1116, 1121, 4134, 40966, 40971, 40975, 40978, 40979, 40981, 40982, 40983, 40984, 40994, 40997, 41000, 41004, 41005.

### A.2 Meta-test UCI Datasets

"acute-inflammations-1", "acute-inflammations-2", "arrhythmia", "balance-scale", "balloons-a", "balloons-b", "balloons-c", "balloons-d", "banknote-authentication", "blood-transfusion-service-center", "breast-cancer-wisconsin-diagnostic", "breast-cancer-wisconsin-original", "breast-cancer-wisconsin-prognostic", "breast-cancer", "car-evaluation", "chess-king-rook-vs-king-pawn", "chess-king-rook-vs-king", "climate-model-simulation-crashes", "cnae-9", "congressional-voting-records", "connectionist-bench-sonar", "connectionist-bench", "contraceptive-method-choice", "credit-approval", "cylinder-bands", "dermatology", "echocardiogram", "ecoli", "fertility", "flags", "glass-identification", "haberman-survival", "hayes-roth", "heart-disease-cleveland", "heart-disease-hungarian", "heart-disease-switzerland", "heart-disease-va", "hepatitis", "hill-valley-noise", "hill-valley", "horse-colic", "image-segmentation", "indian-liver-patient", "ionosphere", "iris", "lenses", "letter-recognition", "libras-movement", "lung-cancer", "magic-gamma-telescope", "mammographic-mass", "monks-problems-1", "monks-problems-2", "monks-problems-3", "mushroom", "nursery", "optical-recognition-handwritten-digits", "ozone-level-detection-eight", "ozone-level-detection-one", "parkinsons", "pen-based-recognition-handwritten-digits", "planning-relax", "poker-hand", "post-operative-patient", "qsar-biodegradation", "seeds", "seismic-bumps", "shuttle-landing-control", "skin-segmentation", "soybean-large", "soybean-small", "spambase", "spect-heart", "spectf-heart", "statlog-project-german-credit", "statlog-project-landsat-satellite", "teaching-assistant-evaluation", "thoracic-surgery", "thyroid-disease-allbp", "thyroid-disease-allhyper", "thyroid-disease-allypo", "thyroid-disease-allrep", "thyroid-disease-ann-thyroid", "thyroid-disease-dis", "thyroid-disease-new-thyroid", "thyroid-disease-sick-euthyroid", "thyroid-disease-sick", "thyroid-disease-thyroid-0387", "tic-tac-toe-endgame", "trains", "wall-following-robot-navigation-2", "wall-following-robot-navigation-24", "wall-following-robot-navigation-4", "wine", "yeast", "zoo".

### A.3 Pipeline Search Space

We build pipelines using scikit-learn [62] primitives. The available components are listed in Table 2. "null" denotes a pass-through.

## APPENDIX B COMMONLY USED META-FEATURES

See Table 3.

## APPENDIX C EXPERIMENT DESIGN FOR WEIGHTED LEAST SQUARES

When factorizing the error matrix by SVD, we approximate performance of different pipelines to different accuracies. Different accuracies can be characterized by different variances in the linear regression model, thus the weighted least squares (WLS) model that would theoretically give the best linear unbiased estimate to the new dataset embedding may perform better.

In detail, recall that the constrained  $D$ -optimal experiment design formulation relies on the assumption that given a low rank matrix multiplication model  $X^T Y = E$ , the error term in linear regression  $\epsilon \sim \mathcal{N}(0, \sigma^2 I)$ , which means each pipeline is predicted to the same accuracy. In the WLS version of our pipeline performance estimation setting, the pipeline performance vector of the new dataset can be written as  $e = Y^T x + \epsilon$ , in which  $\epsilon \sim \mathcal{N}(0, \Sigma)$ .  $\Sigma = \text{diag}(\sigma_1^2, \sigma_2^2, \dots, \sigma_n^2)$  is a covariance matrix; diagonal in the weighted least squares setting. For each pipeline  $j \in [n]$ , we estimate the variance by the sample variance of  $E_{:j} - X^T y_j$ , and show a histogram in Figure 19.

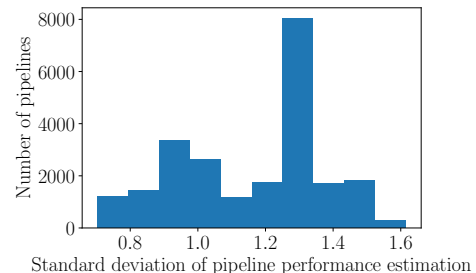


Figure 19: Standard deviation of prediction accuracy of each pipeline, across meta-training datasets.

In this case, the time-constrained  $D$ -experiment design problem to solve becomes

$$\begin{aligned}
 & \text{minimize} && \log \det \left( \sum_{j=1}^n v_j \frac{y_j y_j^T}{\sigma_j^2} \right)^{-1} \\
 & \text{subject to} && \sum_{j=1}^n v_j \hat{t}_j \leq \tau \\
 & && v_j \in \{0, 1\}, \forall j \in [n].
 \end{aligned} \tag{13}$$

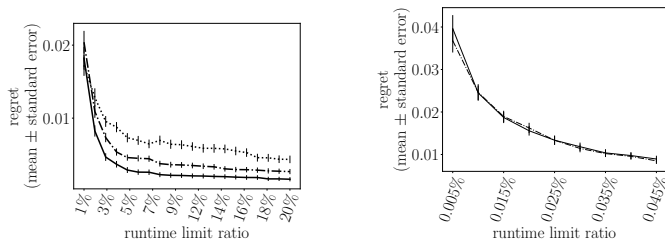
The corresponding greedy approach, which we call *weighted-greedy*, is shown as Algorithm 9. It differs from the ordinary greedy approach in that each  $y_j$  is scaled by  $1/\sigma_j$ . Figure 20 shows its performance compared to convexification and greedy. We can see the weighted-greedy approach performs similarly to the ordinary greedy approach in our experiments.

Table 2: Pipeline search space

Pipeline component	Algorithm type	Hyperparameter names (values)
Missing value imputer	Simple imputer	strategy (mean, median, most_frequent, constant)
Encoder	null	-
	OneHotEncoder	handle_unknown (ignore), sparse (0)
Standardizer	null	-
	StandardScaler	-
Dimensionality reducer	null	-
	PCA	n_components (25%, 50%, 75%)
	VarianceThreshold	-
	SelectKBest	k (25%, 50%, 75%)
Estimator	AdaBoost	n_estimators (50,100), learning_rate (1.0,1.5,2.0,2.5,3)
	Decision tree	min_samples_split (2,4,8,16,32,64,128,256,512,1024,0.01,0.001,0.0001,1e-05)
	Extra trees	min_samples_split (2,4,8,16,32,64,128,256,512,1024,0.01,0.001,0.0001,1e-05), criterion (gini,entropy)
	Gradient boosting	learning_rate (0.001,0.01,0.025,0.05,0.1,0.25,0.5), max_depth (3, 6), max_features (null,log2)
	Gaussian naive Bayes	-
	kNN	n_neighbors (1,3,5,7,9,11,13,15), p (1,2)
	Logistic regression	C (0.25,0.5,0.75,1,1.5,2,3,4), solver (liblinear,saga), penalty (l1,l2)
	Multilayer perceptron	learning_rate_init (0.0001,0.001,0.01), learning_rate (adaptive), solver (sgd,adam), alpha (0.0001, 0.01)
	Perceptron	-
	Random forest	min_samples_split (2,4,8,16,32,64,128,256,512,1024,0.01,0.001,0.0001,1e-05), criterion (gini,entropy)
Linear SVM	C (0.125,0.25,0.5,0.75,1,2,4,8,16)	

Table 3: Dataset Meta-features

Meta-feature name	Explanation
number of instances	number of data points in the dataset
log number of instances	the (natural) logarithm of number of instances
number of classes	
number of features	
log number of features	the (natural) logarithm of number of features
number of instances with missing values	
percentage of instances with missing values	
number of features with missing values	
percentage of features with missing values	
number of missing values	
percentage of missing values	
number of numeric features	
number of categorical features	
ratio numerical to nominal	the ratio of number of numerical features to the number of categorical features
ratio numerical to nominal	
dataset ratio	the ratio of number of features to the number of data points
log dataset ratio	the natural logarithm of dataset ratio
inverse dataset ratio	
log inverse dataset ratio	
class probability (min, max, mean, std)	the (min, max, mean, std) of ratios of data points in each class
symbols (min, max, mean, std, sum)	the (min, max, mean, std, sum) of the numbers of symbols in all categorical features
kurtosis (min, max, mean, std)	
skewness (min, max, mean, std)	
class entropy	the entropy of the distribution of class labels (logarithm base 2)
<b>landmarking [13] meta-features</b>	
LDA	
decision tree	decision tree classifier with 10-fold cross validation
decision node learner	10-fold cross-validated decision tree classifier with criterion='entropy', max_depth=1, min_samples_split=2, min_samples_leaf=1, max_features=None
random node learner	10-fold cross-validated decision tree classifier with max_features=1 and the same above for the rest
1-NN	
PCA fraction of components for 95% variance	the fraction of components that account for 95% of variance
PCA kurtosis first PC	kurtosis of the dimensionality-reduced data matrix along the first principal component
PCA skewness first PC	skewness of the dimensionality-reduced data matrix along the first principal component



(a) Regret on the subsampled error matrix (215-by-183) for estimator search, including the weighted-greedy method.

(b) Regret on the full error matrix (215-by-23424) for pipeline search, including the weighted-greedy method.

⋯|⋯ convexification    + greedy    -| weighted-greedy

Figure 20: Comparison of time-constrained experiment design methods, including the weighted-greedy method.

**Algorithm 9** Greedy algorithm for time-constrained  $D$ -design in WLS setting, with QR initialization

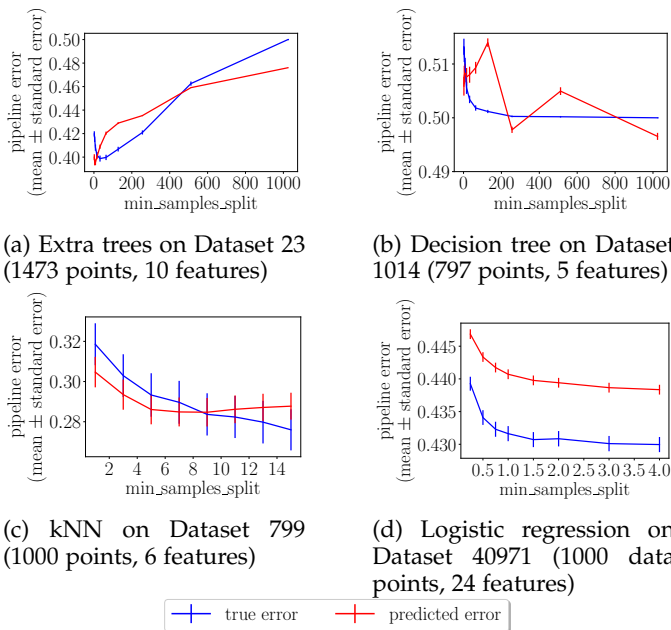
**Input:** design vectors  $\{y_j\}_{j=1}^n$ , in which  $y_j \in \mathbb{R}^k$ ; pipeline estimation variances  $\{\sigma_j^2\}_{j=1}^n$ , (predicted) running time of all pipelines  $\{\hat{t}_i\}_{i=1}^n$ ; maximum running time  $\tau$

**Output:** The selected set of designs  $S \subseteq [n]$

- 1  $y_j \leftarrow y_j / \sigma_j, \forall j \in [n]$
- 2  $S_0 \leftarrow \text{QR\_initialization}(\{y_j\}_{j=1}^n, \{\hat{t}_i\}_{i=1}^n, \tau)$
- 3  $S \leftarrow \text{Greedy\_without\_repetition}(\{y_j\}_{j=1}^n, \{\hat{t}_i\}_{i=1}^n, \tau, S_0)$

## APPENDIX D ZOOMED-IN HYPERPARAMETER LANDSCAPES

See Figure 21.



(a) Extra trees on Dataset 23 (1473 points, 10 features)

(b) Decision tree on Dataset 1014 (797 points, 5 features)

(c) kNN on Dataset 799 (1000 points, 6 features)

(d) Logistic regression on Dataset 40971 (1000 data points, 24 features)

+ true error    + predicted error

Figure 21: Zoomed-in hyperparameter landscapes in Figure 18. The y-axes here do not start from 0.

## APPENDIX E RUNTIME PREDICTION ACCURACY

See Figure 22. Similar plots appeared in our previous KDD version at [12].

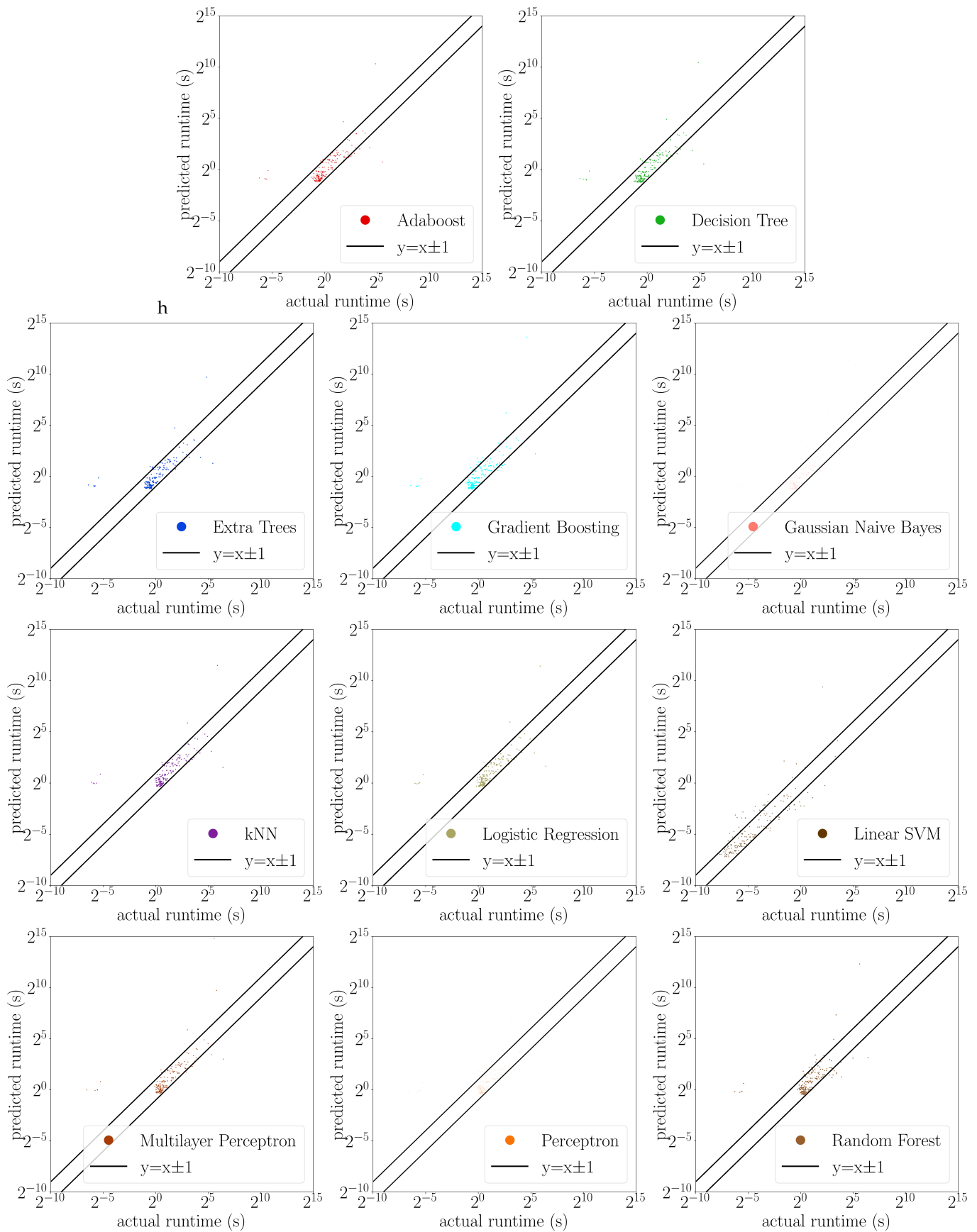


Figure 22: Runtime prediction performance on different machine learning algorithms, on meta-training OpenML datasets.